

# The $\nu_\mu \leftrightarrow \nu_s$ interpretation of the atmospheric neutrino data and cosmological constraints.

Pasquale Di Bari, Paolo Lipari, Maurizio Lusignoli  
 I.N.F.N., Sezione di Roma, and  
 Dipartimento di Fisica, Università di Roma “la Sapienza”,  
 P. A. Moro 2, I-00185 Roma, Italy

October 23, 2019

## Abstract

The data on atmospheric neutrinos can be explained assuming the existence of oscillations between  $\nu_\mu$ 's and a light sterile neutrino with mixing close to maximal, and  $\delta m^2 \sim 3 \times 10^{-3} \text{ eV}^2$ . This interpretation of the data is in potential conflict with the successes of big bang nucleosynthesis (BBN), since oscillations can result in a too large contribution of the sterile state to the energy density of the universe at the epoch of nucleosynthesis. The possibility to evade these cosmological constraints has been recently the object of some controversy. In this work we rediscuss this problem and find that the inclusion of a small mixing of the sterile state with  $\nu_\tau$  can result in the generation of a large lepton asymmetry that strongly suppress the  $\nu_\mu \leftrightarrow \nu_s$  oscillations eliminating the possible conflict with BBN bounds. In this scheme the mass of the tau neutrino must be larger than few eV's and is compatible with cosmological bounds. Our calculations is performed using a Pauli-Boltzmann method. In this approach it is also possible to develop analytic calculations that allow physical insight in the processes considered and give support to the numerical results.

## 1 Introduction

The data on atmospheric neutrinos [1, 2] have shown that muon neutrinos and antineutrinos ‘disappear’ oscillating with a large mixing parameter  $\sin^2 2\theta \simeq 1$  and a squared mass difference  $|\delta m^2| \simeq 3 \times 10^{-3} \text{ eV}^2$  into an ‘invisible’ state. Experimentally this state can be either a  $\tau$  or a sterile neutrino. The existence of light sterile neutrino states is also suggested by the results on solar neutrinos [3] and of the LSND experiment [4] that give independent hints for neutrino oscillations.

If the observed oscillations are into a sterile state, this could have significant cosmological implications, and in fact it has been argued [5, 6, 7] that oscillations with these

parameters are already excluded by the present bounds obtained from primordial nucleosynthesis. Sterile neutrinos not mixed with ordinary neutrinos would have a small average density for temperature  $T \lesssim 100$  MeV, and therefore have a negligible influence during the epoch of nucleosynthesis. However oscillations between sterile and standard neutrinos can be a source of sterile particles, and indeed if the oscillation have sufficiently large amplitude and are sufficiently rapid, the sterile states can be brought in thermal equilibrium with ordinary matter and give a significant contribution to the energy density. The success of Big Bang Nucleosynthesis (BBN) in predicting the relative abundances of primordial nuclear species can be used to put limits on the energy density during the epoch of nucleosynthesis or on the effective number of light particles present during this epoch. For example recently Olive, Steigman and Walker [8] quote a (two sigma) limit  $N_\nu^{\text{eff}} \leq 3.3$ , assuming the so-called low-deuterium option. Such a limit can be translated into an allowed and a forbidden region for the parameters  $\sin^2 2\theta$  and  $\delta m^2$  that describe the oscillations of a sterile neutrino with an ordinary one. Presently there is some controversy on the value of the limit for  $N_\nu^{\text{eff}}$ ; if the limit is relaxed to  $N_\nu^{\text{eff}} \leq 4$ , as someone conservatively supports [9], obviously no region in the neutrino oscillation parameter space can be excluded, however it appears possible that a sterile neutrino in thermal equilibrium with ordinary matter could be excluded by BBN, once the controversial datum on primordial deuterium abundance from high redshift quasar absorbers will be definitely settled [10].

Assume now that  $N_\nu^{\text{eff}} \gtrsim 4$  is excluded by the considerations on nucleosynthesis: does this also exclude the interpretation of the atmospheric neutrino data in terms of  $\nu_\mu \leftrightarrow \nu_s$  oscillations? We will argue here that this is not the case providing an explicit simple model where the cosmological bound is respected.

In this work we will assume that a sterile neutrino state is mixed with the  $\nu_\mu$  with oscillation parameters compatible with the fits to the atmospheric neutrino data, and we will compute the contribution to the energy density at the time of nucleosynthesis due to  $\nu_s$  produced by oscillations. As already found by several authors [5, 6, 7], if the sterile state is only mixed with the  $\nu_\mu$ , for the oscillation parameters suggested by the atmospheric  $\nu$  data, to a good approximation, it is indeed put in thermal equilibrium with the rest of the plasma, and the effective number of neutrinos during nucleosynthesis becomes  $N_\nu^{\text{eff}} \simeq 4$ , in possible conflict with the data on primordial nuclear abundances. It is however remarkable that the density of the sterile state depends critically on the details of its mixing with other ordinary neutrinos. In particular we will show that the inclusion of a very small mixing of the sterile state with the  $\tau$  neutrino ( $\sin^2 2\theta_{\tau s} \simeq 10^{-5}-10^{-9}$ ) can reduce dramatically the energy density of the sterile state to a negligibly small value if the neutrino that is prevalently  $\nu_\tau$  has a mass  $m_\nu \gtrsim 1$  eV. This effect has been demonstrated for the first time by Foot and Volkas [11]. Qualitatively the mechanism that is operating is that  $\nu_\tau \leftrightarrow \nu_s$  oscillations develop earlier in time and generate a net  $\tau$ -lepton number in the plasma that acts to block the  $\nu_\mu \leftrightarrow \nu_s$  oscillations.

This work is organized as follows. In section 2 we describe the effective potential for neutrinos in the hot and dense medium of the early universe and discuss how the oscillation parameters for mixing between standard and ordinary neutrinos are modified by the presence of matter. In section 3 we discuss the method we have used to compute the

evolution with time of the populations of standard and sterile neutrinos. We have chosen in this work not to use the full machinery of the quantum kinetic equations but a simpler (Pauli–Boltzmann) approach, that is approximately valid when the standard neutrino mean free path is much shorter than the oscillation length. In section 4 we will discuss the evolution of the sterile neutrino density in the presence of a two–flavor mixing with a standard neutrino, considering the lepton number per unit comoving volume as constant. In section 5 we rediscuss the two–flavor mixing problem taking into account the fact that since neutrinos and antineutrinos in matter can oscillate with different amplitudes, the oscillations can generate a large lepton number in the medium, that acts back on the oscillations modifying the effective oscillation parameters. In section 6 we discuss the flavor evolution of a system of two standard ( $\nu_\mu$  and  $\nu_\tau$ ) and one sterile neutrino states, and determine the region of oscillation parameters that is in agreement with the  $\nu_\mu \leftrightarrow \nu_s$  interpretation of the atmospheric neutrino data, and also results in a small contribution of sterile neutrinos and anti–neutrinos to the energy density of the universe during nucleosynthesis.

## 2 Effective neutrino mixing in the early universe

We will study the cosmological consequences of assuming the existence of a two-state mixing between two different flavour neutrinos,  $\nu_\alpha$  and  $\nu_\beta$ , with a vacuum mixing angle  $\theta_0$  (defined in the interval  $0 \leq \theta_0 \leq \pi/4$ ) and a squared mass difference  $\delta m^2 = m_b^2 - m_a^2$ . This means that the flavor eigenstates are a linear combination of the mass eigenstates  $\nu_a, \nu_b$  (with well defined masses  $m_a$  and  $m_b$ )

$$|\nu_\alpha\rangle = \cos\theta_0|\nu_a\rangle + \sin\theta_0|\nu_b\rangle, \quad |\nu_\beta\rangle = \cos\theta_0|\nu_b\rangle - \sin\theta_0|\nu_a\rangle. \quad (1)$$

In this way, for ultrarelativistic neutrinos of momentum  $p$  propagating in vacuum, the probability that a state  $|\nu(t)\rangle$  being a pure  $|\nu_\alpha\rangle$  at an initial time  $t_{in}$ , is measured as a  $|\nu_\beta\rangle$  at a time  $t_{in} + \tau$  is:

$$P_0(\nu_\alpha \rightarrow \nu_\beta, t_{in} + \tau) \equiv |\langle \nu_\beta | \nu(t_{in} + \tau) \rangle|^2 = \sin^2 2\theta_0 \cdot \sin^2 \left( \frac{\tau}{2\ell_0(p)} \right) \quad (2)$$

where we defined the vacuum oscillation length as  $\ell_0(p) \equiv 2p/\delta m^2$ . If the neutrinos propagate in matter, the effect of coherent forward scattering of neutrinos with the particles of the medium results in a flavor dependent effective potential that modifies the mixing angle and the oscillation length [12]:

$$\sin^2 2\theta_m(p) = \frac{s^2}{s^2 + (c - v_\alpha(p) + v_\beta(p))^2} \quad (3)$$

$$\ell_m(p) = \frac{\ell_0(p)}{\sqrt{s^2 + (c - v_\alpha(p) + v_\beta(p))^2}} \quad (4)$$

where we introduced the adimensional effective potentials  $v_{\alpha,\beta}(p) \equiv (2p/\delta m^2)V_{\alpha,\beta}$  and we defined  $s \equiv \sin 2\theta_0$ ,  $c \equiv \cos 2\theta_0$ . Consequently, for neutrinos propagating in a homogeneous medium of constant density and composition one has that:

$$P_0(\nu_\alpha \rightarrow \nu_\beta, t_{in} + \tau) \longrightarrow P_m(\nu_\alpha \rightarrow \nu_\beta, t_{in} + \tau) = \sin^2 2\theta_m \cdot \sin^2 \left( \frac{\tau}{2\ell_m(p)} \right) \quad (5)$$

If the condition  $c = v_\alpha(p) - v_\beta(p)$  is satisfied, then a resonance occurs and mixing is maximal [13]. The resonant amplification of the oscillations was first studied in the solar environment where oscillations develop coherently and MSW conversion takes place. In the following we will study the mixing of a standard neutrino ( $\nu_\alpha$  with  $\alpha = e, \mu, \tau$ ) and a strictly sterile neutrino,  $v_\beta = v_s = 0$  in the previous expressions. The effective potential of a standard neutrino depends on its momentum and on the temperature and composition of the medium.

We will study the effect of neutrino oscillations during the time when the universe has a temperature  $T \lesssim 150$  MeV. This is the range of temperatures in which the oscillations can have effects on the products of BBN. The description of neutrino oscillations for higher temperatures and during the quark-hadron phase transition is a difficult problem, in any case the oscillations at high temperature are suppressed by matter effects as it will be discussed in the following. Note also that the population of sterile neutrinos produced by oscillations at high temperature would be afterwards diluted by photon production due to the decrease in the number of degrees of freedom.

We will assume for simplicity that the comoving density of photons is constant, and that the density of muons in the medium is negligible. These assumptions are not exactly correct in the range of temperatures we are considering, but are good approximations. The ratio of the comoving density of muons and electrons  $N_\mu(T)/N_e(T)$  is 0.8 for  $T = m_\mu \simeq 105$  MeV, and drops to 0.1 for  $T \simeq 26$  MeV, as the entropy of the muons is transferred to the other particles of the medium, including the photons. Considering that the statistical weight of muons is about 20% when they are fully present, we can expect that the accuracy of our analysis is 0.02–0.2 for  $25 \lesssim T/\text{MeV} \lesssim 150$ . On the other hand for  $T > 0.5$  MeV  $\simeq m_e$  the variation in the electron particle number can be neglected with a much better accuracy.

The effective potential for a standard neutrino of flavor  $\alpha$  can be written [14, 15] as the sum of two terms

$$v_\alpha(p, T, L^{(\alpha)}) = v_\alpha^L(p, T, L^{(\alpha)}) + v_\alpha^T(p, T) \quad (6)$$

$$= \frac{a_L T^4 y}{\delta m^2} L^{(\alpha)} - \frac{b_\alpha T^6 y^2}{\delta m^2} \quad (7)$$

The effective potential for antineutrinos is obtained changing the sign of the  $v^L$  term, while the  $v^T$  term remains unchanged. Note that in a medium with a net charge number  $L^{(\alpha)}$  neutrinos and anti-neutrinos have different oscillation properties. In equation (7) we have defined  $y = p/T$ , and  $L^{(\alpha)}$  is a linear combination of the charge asymmetries (per photon) of the medium that is relevant for the oscillations of standard neutrinos of flavor

$\alpha$ . For muon neutrinos we have

$$L^{(\mu)} = 2L_{\nu_\mu} + L_{\nu_e} + L_{\nu_\tau} - \frac{1}{2}B_n, \quad (8)$$

where  $Q_x = (n_x - n_{\bar{x}})/n_\gamma$  with  $Q = L$  or  $B$ . In equation (8) we have assumed that the electric charge of the medium vanishes ( $L_e = B_p$ ), and that all particles are in thermal equilibrium with the same temperature  $T$ . The asymmetry relevant for  $\nu_\tau \leftrightarrow \nu_s$  oscillations can be obtained from equation (8) simply interchanging the labels  $\mu$  and  $\tau$ ; for  $L^{(e)}$  one has also to include the contribution of charged current interactions with electrons adding a term  $L_e$ . The constants  $a_L$  and  $b_\alpha$  are:

$$a_L = 2\sqrt{2}G_F \frac{2\zeta(3)}{\pi^2} \simeq 8.014 \times 10^{-12} \text{ MeV}^{-2}, \quad (9)$$

$$b_{\mu(\tau)} = 2\sqrt{2}G_F \left( \frac{8}{3} \frac{1}{M_Z^2} \right) \left( \frac{\pi^2}{15} \frac{7}{8} \right) \simeq 6.10 \times 10^{-21} \text{ MeV}^{-4} \quad (10)$$

and

$$b_e = b_\mu \left( 1 + 2 \frac{M_Z^2}{M_W^2} \right) \simeq 2.17 \times 10^{-20} \text{ MeV}^{-4}. \quad (11)$$

Looking at equations (3) and (7) we can see that if the charge asymmetry of the medium is small, the mixing of neutrinos in matter is strongly suppressed:  $s_m^2 \propto (T^*/T)^{12}$  for temperatures much larger than a characteristic temperature

$$T^*(\delta m^2) = \left( \frac{|\delta m^2|}{b_\alpha} \right)^{\frac{1}{6}}. \quad (12)$$

Numerically we have  $T^* = 23.4$  (18.9)  $|\delta m^2(\text{eV}^2)|^{\frac{1}{6}}$  MeV, for the oscillations of  $\nu_\mu$ 's and  $\nu_\tau$ 's ( $\nu_e$ 's) with sterile neutrinos.

## 2.1 The resonance condition

In the following it will be very important to consider which neutrinos (or anti-neutrinos) have an effective mixing in matter that is maximal. This is verified for  $c - v_\alpha = 0$ , or more explicitly for

$$c \mp \frac{a_L L^{(\alpha)} T^4 y}{\delta m^2} + \frac{b_\alpha T^6 y^2}{\delta m^2} = 0 \quad (13)$$

where the upper (lower) sign applies for neutrinos (anti-neutrinos). This equation is a relation between the temperature  $T$ , the asymmetry  $L^{(\alpha)}$  and the neutrino adimensional momentum  $y = p/T$ . As an illustration in fig. 1 we show for some representative values of the oscillation parameters the set of points in the plane  $(T, L^{(\alpha)})$  for which neutrinos and antineutrinos with adimensional momentum  $y = p/T = 2.2$  (the maximum of the equilibrium Fermi distribution) have maximal mixing.

Except for the special case of maximal mixing in vacuum,  $s^2 = 1$ , it is important to distinguish the cases of  $\delta m^2 > 0$  and  $\delta m^2 < 0$ . A positive (negative)  $\delta m^2$  means that

the mass eigenstate that is prevalently a sterile neutrino is the heavier (lighter) one. If  $\delta m^2 < 0$  (and only in this case) both neutrinos and antineutrinos can have maximal mixing in an exactly symmetric medium ( $L^{(\alpha)} = 0$ ). For neutrinos with adimensional momentum  $y$  this happens at a temperature:

$$T_{\text{res}}^0(y) = \left( \frac{c |\delta m^2|}{b_\alpha y^2} \right)^{\frac{1}{6}} = c^{\frac{1}{6}} T^*(\delta m^2) y^{-\frac{1}{3}} \quad (14)$$

Note that when the temperature decreases, neutrinos with higher and higher momentum  $y \propto T^{-3}$  are resonant. More in general (always in the case  $\delta m^2 < 0$ ), given a certain value of the temperature  $T$ , for a non vanishing value of the asymmetry  $L^{(\alpha)}$ , neutrinos and anti-neutrinos have maximal mixing for different adimensional momenta. One has:

$$y_{\nu_\alpha(\bar{\nu}_\alpha)}^{\text{res}} = \pm \frac{1}{2} \frac{a_L}{b_\alpha} \frac{L^{(\alpha)}}{T^2} + \frac{1}{2} \sqrt{\left( \frac{a_L}{b_\alpha} \frac{L^{(\alpha)}}{T^2} \right)^2 + 4c \frac{|\delta m^2|}{b_\alpha} \frac{1}{T^6}} \quad (15)$$

For a neutral medium the two values coincide, for  $L^{(\alpha)} > 0$  one has  $y_{\nu_\alpha}^{\text{res}} > y_{\bar{\nu}_\alpha}^{\text{res}}$ , and the opposite for  $L^{(\alpha)} < 0$ . For large asymmetries of the medium the expressions for the resonant values of the adimensional momenta take the asymptotic forms:

$$y_{\text{high}}^{\text{res}} = \frac{a_L}{b_\alpha} \frac{|L^{(\alpha)}|}{T^2} \quad (16)$$

and

$$y_{\text{low}}^{\text{res}} = \frac{c |\delta m^2|}{a_L |L^{(\alpha)}| T^4}. \quad (17)$$

For  $L^{(\alpha)}$  positive  $y_{\text{high}}^{\text{res}}$  applies to neutrinos and  $y_{\text{low}}^{\text{res}}$  to anti-neutrinos and vice versa for  $L^{(\alpha)}$  negative.

In the case of  $\delta m^2 > 0$ , the situation of maximal mixing can be present only for neutrinos or antineutrinos (but not for both), and this is possible only for a sufficiently large charge asymmetry of the medium. The resonance condition is verified for neutrinos (antineutrinos) only for  $L^{(\alpha)} > L^*$  ( $L^{(\alpha)} < -L^*$ ) where

$$L^* = \frac{2 \sqrt{c b_\alpha \delta m^2}}{a_L T} \quad (18)$$

If this condition is satisfied the neutrinos (anti-neutrinos) have resonant mixing for two values of the momentum given by

$$y_{\nu_\alpha(\bar{\nu}_\alpha)}^{\text{res}} = + \frac{1}{2} \frac{a_L}{b_\alpha} \frac{|L^{(\alpha)}|}{T^2} \pm \frac{1}{2} \sqrt{\left( \frac{a_L}{b_\alpha} \frac{L^{(\alpha)}}{T^2} \right)^2 - 4c \frac{\delta m^2}{b_\alpha} \frac{1}{T^6}} \quad (19)$$

(the  $\pm$  gives the two solutions for either neutrinos or anti-neutrinos).

In the case of  $s^2 = 1$ , the sign of  $\delta m^2$  is not well defined, and the resonant condition can be obtained as the limit  $c \rightarrow 0$  from both the solutions found for positive or negative

$\delta m^2$ . Effective maximal mixing in matter is obviously present for both neutrinos and antineutrinos for  $y = 0$ , for any conditions of the medium, since in this situation all matter effects vanish; a second resonant value of the adimensional momentum  $y^{\text{res}} = (a_L/b_\mu)(|L^{(\alpha)}|/T^2)$  exists for neutrinos (for  $L^{(\alpha)} > 0$ ) or anti-neutrinos (for  $L^{(\alpha)} < 0$ ).

Some examples of the dependence on the momentum  $y$  of the mixing parameter in matter are shown in fig. 14, to be discussed in section 6. It is important to note that for a given condition of the medium (fixing the temperature and quantum numbers of the plasma) the width of the resonance, that is the momentum range for which neutrinos or antineutrinos have a large mixing is in general very narrow ( $\delta y/y \ll 1$ ) and only a small fraction of all neutrino momenta can oscillate efficiently. Note also that the neutrinos have a non-negligible population only for values of  $y$  not too far from  $y_{\text{peak}} \simeq 2.2$ , and therefore if the resonant momentum is  $y_{\nu_\alpha(\bar{\nu}_\alpha)}^{\text{res}} \ll 0.1$  or  $y_{\nu_\alpha(\bar{\nu}_\alpha)}^{\text{res}} \gg 10$  the resonance has little practical importance.

Because of the narrowness of the resonant regions it is essential to study the flavor evolution of the neutrino ensembles considering in detail the momentum distribution of the particles. The approximation of considering monochromatic neutrino populations with a single momentum  $p = \langle p \rangle$  does not give a sufficiently accurate description of the problem.

### 3 Kinetic equations for the sterile and active neutrino distributions

A rigorous description of the flavor evolution of the ensemble of neutrinos in the early universe has to take into account at the same time the quantum coherent effects of oscillations and the effects of interactions with the particles of the dense medium. This can be done rigorously making use of a density matrix formalism [16]. The interactions result in a loss of quantum coherence for the neutrinos [17, 18]. It is possible to write the reduced density matrix for a system of two mixed neutrino flavors in the form

$$\rho(p) = \frac{1}{2} [P_0(p)I + \mathbf{P}(p) \cdot \boldsymbol{\sigma}] \quad (20)$$

where  $\sigma_j$  ( $j = 1, 2, 3$ ) are the Pauli matrices and  $\mathbf{P} = (P_1, P_2, P_3)$  is a vector. The diagonal entries of  $\rho$  are the ratios of the classical distribution function ( $f_{\nu_\alpha}(p)$  for  $\nu_\alpha$  and  $f_{\nu_s}(p)$  for  $\nu_s$ ) with the zero chemical potential Fermi-Dirac distribution  $f_{eq}^0(p) \equiv 1/[1 + \exp(p/T)]$ , so that:

$$P_z(p) = \frac{f_{\nu_\alpha}(p) - f_{\nu_s}(p)}{f_{eq}^0(p)} \quad P_0(p) = \frac{f_{\nu_\alpha}(p) + f_{\nu_s}(p)}{f_{eq}^0(p)} \quad (21)$$

Starting from first principles it is possible to derive [19] the following set of equations for  $\mathbf{P}$  and  $P_0$ , dubbed quantum kinetic equations (QKE):

$$\frac{d}{dt}\mathbf{P}(\tilde{p}, t) = \mathbf{V}(\tilde{p}, t) \wedge \mathbf{P}(\tilde{p}, t) - D(\tilde{p}, t)\mathbf{P}_T(\tilde{p}, t) + \frac{d}{dt}P_0(\tilde{p}, t)\hat{z} \quad (22)$$

$$\frac{d}{dt}P_0(\tilde{p}, t) = R(\tilde{p}, t) \quad (23)$$

where:

$$\mathbf{P}_T = P_x \hat{x} + P_y \hat{y} \quad (24)$$

$$\mathbf{V} = V_x \hat{x} + V_y \hat{y} + V_z \hat{z} \quad (25)$$

$$V_x = \frac{\delta m^2}{2p} s, \quad V_y = 0, \quad V_z = \frac{\delta m^2}{2p} [c - v_\alpha(p, t)] \quad (26)$$

Analogous relations hold for antineutrinos.

The use of *local momenta*  $\tilde{p} \equiv p (R/R_*)$  ( $R$  is the scale factor,  $R_*$  its reference value at a temperature  $T_*$ ) in the evolution equations (22) allows to take into account the expansion of the universe avoiding the explicit presence of a partial derivative term in the left hand sides (see for example [20]). As we are dealing with constant photon number,  $R/R_* = T_*/T$  and thus we can use the convenient adimensional momentum  $y \equiv p/T$ .

The first term in the right hand side of equation (22) describes the coherent evolution of mixed neutrinos, while the second term describes the decoherence effect of interactions through a *damping function*  $D(y)$  that has the simple expression [21]:

$$D(y) = \frac{1}{2} \Gamma_\alpha(y), \quad (27)$$

where

$$\Gamma_\alpha(y) = G_F^2 k_\alpha T^5 y \quad (28)$$

is the total collision rate for an active neutrino  $\nu_\alpha$  with momentum  $p = yT$  and  $k_\alpha \simeq 0.92$  (1.27) for  $\alpha = \mu, \tau$  ( $\alpha = e$ ). In equation (28) we have neglected Pauli blocking factors, and assumed that the charge asymmetry of the medium is negligible. Correction terms for the presence of asymmetries in the neutrino lepton number are given in [21] and are small. With this assumption the damping functions for neutrinos and anti-neutrinos are equal. It is also convenient to introduce an adimensional damping function:

$$d_\alpha(y) \equiv \frac{2p}{|\delta m^2|} D(y) = \frac{G_F^2 k_\alpha T^6 y^2}{|\delta m^2|}. \quad (29)$$

The third term  $(dP_0/dt)\hat{z}$  in equation (22) takes into account the variation of the total number of standard plus sterile neutrinos. This happens because, while  $\nu_\alpha$  oscillate producing  $\nu_s$ , the inelastic collisions refill the quantum  $\nu_\alpha$  states to preserve chemical equilibrium and this effect changes only the  $z$ -component. The *repopulation function*  $R(y)$ , driving the evolution of  $P_0$ , for  $T \gtrsim 1$  MeV has the form [21]:

$$R(y) \simeq \Gamma_\alpha(y) \left\{ \frac{f_{eq}^{\xi_\alpha}(y) - f_{\nu_\alpha}(y)}{f_{eq}^0(y)} \right\}. \quad (30)$$

In equation (30),  $f_{eq}^{\xi_\alpha} \equiv 1/[1 + \exp(y - \xi_\alpha)]$  is the Fermi-Dirac distribution and  $\xi_\alpha \equiv \mu_\alpha/T$  is the adimensional chemical potential; the approximation symbol means that the



expression is rigorously true only in the limit of complete thermal equilibrium for the non oscillating particles. When the average collision rate is much larger than the expansion rate of the universe  $H(T)$ , the deviations from equilibrium are so small that the term  $(dP_0/dt)\hat{z}$  can be neglected and equation (22) becomes a *damped Bloch equation*, well-known in studies of nuclear and electronic spin motion. An important thing to notice is that the initial condition of the system is necessarily  $\mathbf{P}_T = 0, P_0 = 1$ , because at high enough temperatures the damping parameter would be always so high to destroy any transversal component (*Turing or Zeno Paradox*) [17] and because the presence of sterile neutrinos is initially negligible. In fact a sterile neutrino decouples at very early times when  $T \gg 100$  GeV and thus its density is highly diluted by the subsequent disappearance of degrees of freedom, especially at the quark-hadron phase transition.

In this work, to study the flavor evolution of the ensemble of neutrinos, we will use a simpler set of equations that is given below:

$$\frac{d}{dt}f_{\nu_s}(y, t) = \Gamma_{\alpha s}(y) \cdot [f_{\nu_\alpha}(y, t) - f_{\nu_s}(y, t)] \quad (31)$$

$$\frac{d}{dt}f_{\bar{\nu}_s}(y, t) = \bar{\Gamma}_{\alpha s}(y) \cdot [f_{\bar{\nu}_\alpha}(y, t) - f_{\bar{\nu}_s}(y, t)] \quad (32)$$

$$\frac{d}{dt}f_{\nu_\alpha}(y, t) = \Gamma_{\alpha s}(y) \cdot [f_{\nu_s}(y, t) - f_{\nu_\alpha}(y, t)] + \sum_r C_r[f_{\nu_\alpha}] \quad (33)$$

$$\frac{d}{dt}f_{\bar{\nu}_\alpha}(y, t) = \bar{\Gamma}_{\alpha s}(y) \cdot [f_{\bar{\nu}_s}(y, t) - f_{\bar{\nu}_\alpha}(y, t)] + \sum_{\bar{r}} C_{\bar{r}}[f_{\bar{\nu}_\alpha}] \quad (34)$$

where [11]:

$$\Gamma_{\alpha s}(y) = \frac{\Gamma_\alpha}{2} s_m^2 \left[ 1 + \left( \frac{\Gamma_\alpha \ell_m}{2} \right)^2 \right]^{-1} = \frac{1}{4} \frac{\Gamma_\alpha(y) \cdot s^2}{s^2 + d_\alpha^2(y) + [c - v_\alpha^T(y) - v_\alpha^L(y)]^2} \quad (35)$$

$$\bar{\Gamma}_{\alpha s}(y) = \frac{\Gamma_\alpha}{2} \bar{s}_m^2 \left[ 1 + \left( \frac{\Gamma_\alpha \bar{\ell}_m}{2} \right)^2 \right]^{-1} = \frac{1}{4} \frac{\Gamma_\alpha(y) \cdot s^2}{s^2 + d_\alpha^2(y) + [c - v_\alpha^T(y) + v_\alpha^L(y)]^2} \quad (36)$$

(for the explicit form in the right-hand side we have used the fact that  $s_m^2/\ell_m^2 = s^2/\ell_0^2$  and the definition (29) for  $d_\alpha$ ). The  $C_r[ ]$  in equations (33) and (34) are the collisional operators [20] for the different reactions involving the standard neutrinos and other particles in the medium. This set of equations can be rigorously derived from the quantum kinetic equations (QKE) under an appropriate set of approximations, as first discussed in [22, 11] and shown in great detail in [21].

The equations have a simple probabilistic interpretation, and can be derived with heuristic considerations [23, 11]. Active and sterile neutrinos are described as two different particle species and oscillations work as a special inelastic process that can transform an active neutrino into a sterile neutrino and vice versa. The rate for the flavor transitions ( $\alpha \rightarrow s$  or  $s \rightarrow \alpha$ ) can be derived considering oscillations that develop only between

interactions (or “measurement processes”) that happen with an average time interval  $\tau = 2/\Gamma_\alpha$  (see [11] for a more detailed discussion). From these considerations one obtains:

$$\Gamma_{\alpha s} = \Gamma_{s\alpha} = \frac{\Gamma_\alpha(y)}{2} \langle P_m(\nu_\alpha \rightarrow \nu_s, t_{in} + \tau) \rangle_\tau = \frac{\Gamma_\alpha(y)}{2} s_m^2 \left[ 1 + \left( \frac{\Gamma_\alpha \ell_m}{2} \right)^2 \right]^{-1}. \quad (37)$$

The solution of the flavor evolution equations is greatly simplified assuming that the standard neutrinos remain in chemical equilibrium. The effect of the collisional operators for sufficiently large temperature, i.e. for  $T \gtrsim 3.5$  (2.5) MeV for  $\alpha = \mu, \tau$  ( $\alpha = e$ ), is in fact to maintain, to a very good approximation, in thermal and chemical equilibrium the population of standard neutrinos. The elastic reactions redistribute the lepton number in a thermal way and the inelastic processes refill continuously the quantum states depleted by the oscillations.

The assumption of thermal equilibrium for the standard neutrinos does not determine completely their momentum distributions, because in general  $\nu$ 's and  $\bar{\nu}$ 's have different oscillation probabilities; this can generate an asymmetry in the lepton number  $L_{\nu_\alpha}$  (that cannot be cancelled by collisions) and a non vanishing chemical potential. The following relation connects the lepton number  $L_{\nu_\alpha}$  to the adimensional chemical potentials for neutrinos and anti-neutrinos:

$$L_{\nu_\alpha} = \frac{1}{n_\gamma} \int \frac{d^3p}{(2\pi)^3} \left( \frac{1}{e^{y-\xi_\alpha} + 1} - \frac{1}{e^{y-\bar{\xi}_\alpha} + 1} \right), \quad (38)$$

which for  $\xi_\alpha, \bar{\xi}_\alpha \ll 1$  becomes simply:

$$L_{\nu_\alpha} = \frac{\pi^2}{24 \zeta(3)} (\xi_\alpha - \bar{\xi}_\alpha) + \mathcal{O}(\xi_\alpha^2, \bar{\xi}_\alpha^2) \quad (39)$$

If the standard neutrinos are in thermal equilibrium one has  $\bar{\xi}_\alpha = -\xi_\alpha$  and the active neutrino distributions are described only through  $L_{\nu_\alpha}$ . Below the chemical decoupling temperature this is not true in general and one should take into account also the quantity  $\xi_\alpha + \bar{\xi}_\alpha$ : this is important if one wants to describe the effects of electron chemical potentials on BBN [24]. For the temperatures relevant for our discussion chemical equilibrium is verified, and therefore these effects are not important and we will make the approximation that a single quantity  $L_{\nu_\alpha}$  fully determines the momentum distributions of both neutrinos and anti-neutrinos of flavor  $\alpha$ .

A detailed discussion of the conditions for which the framework we are using gives a good description of the flavor evolution of neutrinos in the early universe can be found in [21]. Here we will give only some simple remarks. There is a small angle condition, that away from resonances is simply

$$s^2 \ll 1. \quad (40)$$

Near to a resonance, the constraint is generally more restrictive:

$$s^2 \ll d_\alpha^2(y) \Big|_{T=T_{\text{res}}(y)} = 4.0 (0.64) 10^{-4} c^2 \left( \frac{T_{\text{res}}}{T_{\text{res}}^0} \right)^{12} \quad (41)$$

for  $\alpha = \mu, \tau$  ( $\alpha = e$ ), where  $T_{\text{res}}(y)$  also depends on  $L^{(\alpha)}$ . For  $L^{(\alpha)} = 0$ ,  $T_{\text{res}}(y) = T_{\text{res}}^0(y)$ , defined by equation (14). These conditions assure that the transversal components of the vectors  $\mathbf{P}$  and  $\overline{\mathbf{P}}$  remain small and have a negligible effect on the evolution of the diagonal terms of the density matrix  $\rho$ .

For a qualitative understanding it is useful to consider the ratio of the mean distance between two collisions (or we could say two measuring processes [18]) and the oscillation length (in matter), that has the following expression:

$$\frac{\ell_{int}}{\ell_m} = \frac{\sqrt{s^2 + (c - v_\alpha)^2}}{d_\alpha}. \quad (42)$$

Far from the resonance (both above,  $|v_\alpha| \gg c$ , and below,  $|v_\alpha| \ll c$ ), it is easily seen that this ratio is always much greater than 1 and oscillations develop coherently. In this case the condition  $s^2 \ll 1$  assures that the amplitude of the oscillations is not too large and that the vector  $\mathbf{P}$  remains close to the  $\hat{z}$ -axis. At the resonance however the mixing is maximal and a coherent evolution would anyhow create a large transversal component. Here one has therefore to impose that the oscillations do not develop coherently and this corresponds to require  $s/d_\alpha \ll 1$ , equation (41).

Together with the small angle condition, one should also require that the effective potential and the damping function remain approximately constant between two collisions, otherwise the diagonal terms of the density matrix have still an appreciable dependence on the derivatives of the off-diagonal terms. In [21] it is shown that the parameter variation is maximal at the resonance and that the (most restrictive) condition assumes the form  $D \gtrsim 6H$ . This condition implies that in order to be confident in the approximation the bulk of (anti-)neutrinos should enter the resonance at a temperature  $T_{\text{res}} \gtrsim 3 \text{ MeV}$ . If the charge number is negligible this implies that the Pauli-Boltzmann approach can be used only for  $|\delta m^2| > 10^{-5} \text{ eV}^2$ , see equation (14). For  $T \lesssim 3 \text{ MeV}$ , full MSW conversion can occur at the resonance, an effect that the Pauli-Boltzmann approach neglects. In this situation major differences from a full quantum approach are expected.

One could observe that the  $s^2$  term should be neglected in the denominators of equations (35) and (36) to be coherent with the condition  $s/d_\alpha \ll 1$ . If this condition does not hold we should expect uncorrect results for the calculation of lepton number evolution in a Pauli-Boltzmann approach. However, even in presence of a large transversal component we may obtain reasonable results (provided that full MSW conversion does not occur) for the calculation of sterile neutrino contribution to the effective number of neutrinos, in which the sum of neutrino and antineutrino distributions enters. In fact the motion of  $\mathbf{P}$  around the  $\hat{z}$ -axis represents only a deviation from the mean value and will be much less important in the sum (effective number of sterile neutrinos) than in the difference (lepton asymmetries): this is also visible in the figures shown in [15].

It is thus meaningful to extend the classic approach also to high values of mixing angle. To this purpose we will keep the term  $s^2$  in the denominators. In [21], proceeding directly from QKE, expressions for the rates that do not contain this term have been obtained. As we will see in next section, this would spoil the nice agreement of the results that we obtain using a Pauli-Boltzmann approach with those obtained using the QKE.

For the lepton asymmetry evolution the differences are more relevant and a classic approach misses the oscillatory behaviour at large angles [15, 22, 25] (of course below 3 MeV it also neglects MSW conversion effect on the lepton asymmetry evolution).

## 4 Sterile $\nu$ production for constant $L^{(\alpha)}$ .

In the previous section we have reduced the problem of the evolution of the ensemble of neutrinos in the early universe to the solution of a set of coupled differential equations. The flavor transition rates  $\Gamma_{\alpha s}$  and  $\bar{\Gamma}_{\alpha s}$  depend on the lepton number  $L_{\nu_\alpha}$  that is determined by the oscillation themselves, and therefore we have a non-linear problem. In this section we will begin solving a simpler problem considering the asymmetry  $L_{\nu_\alpha}$  as constant. We will show that in the framework of our method, the solution of this problem can be expressed in a very simple form. In the next section we will discuss the complete problem and consider the lepton number as a dynamical variable.

The first step for the calculation is to rearrange the equations in a more convenient form, replacing the distribution functions with the following quantities:

$$z_s \equiv \frac{f_{\nu_s}}{f_{eq}^0} \quad \bar{z}_s \equiv \frac{f_{\bar{\nu}_s}}{f_{eq}^0} \quad (43)$$

As we will deal with small chemical potentials ( $\bar{\xi}_\alpha, \xi_\alpha \ll 1$ ), we can perform the expansion:

$$f_{\nu_\alpha}(y) = f_{eq}^0 \left( 1 + \xi_\alpha \frac{e^y}{e^y + 1} + \mathcal{O}(\xi_\alpha^2) \right) \quad (44)$$

Moreover, considering that the equilibrium distribution  $f_{eq}^0$  satisfies the Boltzmann equation (see e.g. [20]):

$$L[f_{eq}^0] \equiv \frac{\partial}{\partial t} f_{eq}^0(p, t) - pH \frac{\partial}{\partial p} f_{eq}^0(p, t) \equiv \frac{d}{dt} f_{eq}^0(y, t) = 0, \quad (45)$$

it is easy to derive from equations (31) and (32), the following equations for  $z_s(y, t)$ ,  $\bar{z}_s(y, t)$  (neglecting terms  $\mathcal{O}(\xi_\alpha^2)$ ):

$$\frac{d}{dt} z_s(y, t) = \Gamma_{\alpha s}(y, t) \left[ 1 - z_s(y, t) + \xi_\alpha(t) \frac{e^y}{e^y + 1} \right] \quad (46)$$

$$\frac{d}{dt} \bar{z}_s(y, t) = \bar{\Gamma}_{\alpha s}(y, t) \left[ 1 - \bar{z}_s(y, t) + \bar{\xi}_\alpha(t) \frac{e^y}{e^y + 1} \right] \quad (47)$$

We are interested to calculate the contribution of sterile neutrinos to the energy density of the universe. For this purpose it is usual to define a sterile neutrino effective number:

$$N_{\nu_s}^{\text{eff}} \equiv \frac{\rho_{\nu_s} + \rho_{\bar{\nu}_s}}{2 \rho_{eq}^0} \quad (48)$$

where  $\rho_{eq}^0 = (7/8)(\pi^2/30)T^4$  is the energy density per degree of freedom of a fermion particle in thermal equilibrium with vanishing chemical potential. The results on BBN can be used to put constraints on this quantity at a temperature  $T \lesssim 1$  MeV. The sterile neutrino effective number can be expressed as:

$$N_{\nu_s}^{\text{eff}} = \frac{120}{7\pi^4} \int dy \frac{y^3}{1+e^y} z_s^+(y) \quad (49)$$

where  $z_s^+ \equiv (z_s + \bar{z}_s)/2$ . It is also interesting to consider the sterile neutrino charge number  $L_{\nu_s} \equiv (n_{\nu_s} - n_{\bar{\nu}_s})/n_\gamma$ :

$$L_{\nu_s} = \frac{1}{2\zeta(3)} \int dy \frac{y^2}{1+e^y} z_s^-(y) \quad (50)$$

where  $z_s^- \equiv (z_s - \bar{z}_s)/2$ . Thus we see that the interesting quantities to be calculated are  $z_s^+$  and  $z_s^-$ , also because, when dealing with the coupled problem, these will be the quantities entering the equation for the  $\alpha$ -neutrino lepton number. We can derive from equations (46) and (47) the evolution equations for  $z_s^+$  and  $z_s^-$ , using  $\xi_\alpha = -\bar{\xi}_\alpha$ :

$$\frac{dz_s^+}{dt} = \frac{\Gamma_{\alpha s} + \bar{\Gamma}_{\alpha s}}{2} [1 - z_s^+] + \frac{\Gamma_{\alpha s} - \bar{\Gamma}_{\alpha s}}{2} \left[ \xi_\alpha \frac{e^y}{e^y + 1} - z_s^- \right] \quad (51)$$

$$\frac{dz_s^-}{dt} = \frac{\Gamma_{\alpha s} - \bar{\Gamma}_{\alpha s}}{2} [1 - z_s^+] + \frac{\Gamma_{\alpha s} + \bar{\Gamma}_{\alpha s}}{2} \left[ \xi_\alpha \frac{e^y}{e^y + 1} - z_s^- \right] \quad (52)$$

From equations (35) and (36) and using the definition  $v_\alpha^L = \tilde{v}(y, T) L^{(\alpha)}$ , is easy to find the following expressions:

$$\Gamma_{\alpha s} - \bar{\Gamma}_{\alpha s} = \frac{s^2 \Gamma_\alpha}{\Delta} \cdot \tilde{v}(c - v_\alpha^T) \cdot L^{(\alpha)}, \quad (53)$$

$$\Gamma_{\alpha s} + \bar{\Gamma}_{\alpha s} = \frac{1}{2} \frac{s^2 \Gamma_\alpha}{\Delta} \cdot [s^2 + d_\alpha^2 + (c - v_\alpha^T)^2 + (v_\alpha^L)^2], \quad (54)$$

with

$$\Delta \equiv [s^2 + d_\alpha^2 + (c - v_\alpha^T - v_\alpha^L)^2] \cdot [s^2 + d_\alpha^2 + (c - v_\alpha^T + v_\alpha^L)^2]. \quad (55)$$

These equations allow to show that the terms explicitly containing  $\xi_\alpha$  can be safely neglected: in the equation (51) the term containing  $\xi_\alpha$  is actually an  $\mathcal{O}(\xi_\alpha^2)$  term, while in the equation (52) the analogous term gives a small correction because  $[s^2 + d_\alpha^2 + (c - v_\alpha^T)^2 + (v_\alpha^L)^2] \ll \tilde{v}(y, T)[c - v_\alpha^T(y, T)]$  for the relevant values of  $y$  and in the range of temperatures we are considering. Thus we can neglect the  $\xi_\alpha$  terms in the equations for  $z_s$  (46) and  $\bar{z}_s$  (47).

It is convenient to adopt as independent variable in these equations the temperature instead of the time, using:

$$\frac{dT}{dt} = -H(T) T = -\frac{\alpha_H T^2}{M_P} T \quad (56)$$

where  $M_P$  is the Planck mass and

$$\alpha_H = \sqrt{\frac{\pi^2}{30} \frac{43}{4} \frac{8\pi}{3}} \simeq 5.44 . \quad (57)$$

One obtains in this way [11]:

$$\frac{d}{dT} z_s(y, T) = -\frac{\Gamma_{\alpha s}(y, T)}{H(T)T} [1 - z_s(y, T)] \quad (58)$$

$$\frac{d}{dT} \bar{z}_s(y, T) = -\frac{\bar{\Gamma}_{\alpha s}(y, T)}{H(T)T} [1 - \bar{z}_s(y, T)] . \quad (59)$$

These equations are now simple enough to allow analytic solutions for the different parameters involved (lepton number included). It is convenient to write the solution in the following form [26]:

$$z_s(y, T) \equiv \frac{f_{\nu_s}(y, T)}{f_{e q}^0(y)} = 1 - \exp[-g_s(y, T)] . \quad (60)$$

The function  $g_s(y, T)$ , assuming that the asymmetry is constant in time, can be calculated with a simple integral:

$$g_s(y, T) = \int_T^\infty dT' \frac{\Gamma_{\alpha s}(y, T')}{H(T')T'} . \quad (61)$$

For  $\bar{z}_s$  and  $\bar{g}_s$  one has simply to make the substitution  $\Gamma_{\alpha s} \rightarrow \bar{\Gamma}_{\alpha s}$ . Using the definitions of  $\Gamma_{\alpha s}$  and  $H(T)$  one can write more explicitly:

$$g_s(y, T) = K_\alpha |\delta m^2|^{\frac{1}{2}} s^2 G_{\nu_s}(y, T) , \quad (62)$$

with a similar expression for anti-neutrinos. In equation (62) we defined

$$K_\alpha = \frac{G_F^2 k_\alpha M_P}{4 b_\alpha^{\frac{1}{2}} \alpha_H} \simeq 898 (657) \text{ eV}^{-1} \quad (63)$$

for  $\alpha = \mu, \tau$  ( $\alpha = e$ ), and the function  $G_{\nu_s}(y, T)$ , that depends on the parameters  $s^2$ ,  $\delta m^2$  and  $L^{(\alpha)}$  :

$$G_{\nu_s}(y, T) = \int_{T/\bar{T}(y, \delta m^2)}^\infty dt \frac{t^2}{s^2 + d_0^2 t^{12} + \left[ c \mp a_L b_\alpha^{-\frac{2}{3}} L^{(\alpha)} |\delta m^2|^{-\frac{1}{3}} y^{-\frac{1}{3}} t^4 \pm t^6 \right]^2} \quad (64)$$

In equation (64) the upper (lower) signs hold for  $\delta m^2 > 0$  ( $\delta m^2 < 0$ ), and the constant  $d_0$  is given by

$$d_0 = \frac{G_F^2 k_\alpha}{b_\alpha} \simeq 0.02 (0.008) \text{ for } \alpha = \mu, \tau (\alpha = e) . \quad (65)$$

The function  $G_{\bar{\nu}_s}$  is obtained changing the sign of the term containing  $L^{(\alpha)}$ . In the lower limit of integration we have introduced the definition:

$$\bar{T}(y, \delta m^2) = \left( \frac{|\delta m^2|}{b_\alpha y^2} \right)^{\frac{1}{6}}. \quad (66)$$

We are interested in the limit of small  $T$ , i.e. generally  $T < \bar{T}(y, \delta m^2)$  (for typical  $y$  values). Note that for  $\delta m^2 < 0$  and in the absence of asymmetry, neutrinos and anti-neutrinos with adimensional momentum  $y$  have maximal mixing at  $T = c^{\frac{1}{6}} \bar{T}(y, \delta m^2)$ , see equation (14).

#### 4.1 Vanishing charge asymmetry of the medium

It is interesting to consider first the case where the charge asymmetry of the medium is negligibly small. In this case the population of sterile neutrinos and anti-neutrinos created by the oscillations are identical. For  $L^{(\alpha)} = 0$  equation (64) simplifies to

$$G_{\nu_s(\bar{\nu}_s)}^\pm(y, T) = \int_{T/\bar{T}(y, \delta m^2)}^\infty dt \frac{t^2}{s^2 + d_0^2 t^{12} + (c \pm t^6)^2} \quad (67)$$

where the positive (negative) sign refer to  $\delta m^2 > 0$  ( $\delta m^2 < 0$ ), while neutrinos and anti-neutrinos have the same distribution. Note that all dependence on  $|\delta m^2|$  and  $y$  is in the value of the lower limit of integration. For  $T \rightarrow 0$  the dependences on  $y$  and  $|\delta m^2|$  disappear and the function  $G$  depends only on the mixing parameter  $s^2$ .

$$\lim_{T \rightarrow 0} G_{\nu_s(\bar{\nu}_s)}^\pm(y, T) = F_\pm(s^2) = \int_0^\infty dt \frac{t^2}{s^2 + d_0^2 t^{12} + (c \pm t^6)^2} \quad (68)$$

the  $\pm$  sign again refers to the cases of positive or negative  $\delta m^2$ .

In fig. 2 we plot the functions  $F_\pm(s^2)$ . For maximal mixing the two curves have the same value ( $F_\pm(1) \simeq \pi/(6\sqrt{2}) \simeq 0.37$ ), while for  $s^2 \lesssim 10^{-4}$  the two functions tend to values that differ by approximately two orders of magnitude ( $F_-(0) \simeq 25.3$ ,  $F_+(0) \simeq 0.26$ ). This is easily understood noting that for  $\delta m^2 < 0$  and  $L^{(\alpha)} = 0$ , both neutrinos and anti-neutrinos with adimensional momentum  $y$  go through a resonance for a brief time interval when the temperature is close to the value  $c^{\frac{1}{6}} \bar{T}(y, \delta m^2)$ , while in the case of positive  $\delta m^2$  the resonance is absent.

Most of the production of the sterile neutrinos for the case  $\delta m^2 < 0$  happens during the short time when maximal mixing is produced. This is illustrated in fig. 3 that shows one example of the evolution of the sterile neutrino population for negative  $\delta m^2$ . The fact that the final momentum distribution of the sterile neutrinos is proportional to a thermal distribution is the non trivial effect of an exact cancellation between the amount of time that each momentum spends at the resonance, and the degree of damping of the oscillations due to the interactions.

Note that in the plane  $(s^2, \delta m^2)$ , a line of constant  $N_{\nu_s}^{\text{eff}}$  can be obtained from

$$N_{\nu_s}^{\text{eff}} = 1 - \exp \left[ -K_\alpha |\delta m^2|^{\frac{1}{2}} s^2 F_\pm(s^2) \right]. \quad (69)$$

For small  $s^2$  the corresponding line is:

$$|\delta m^2|^{\frac{1}{2}} s^2 = -\frac{1}{K_\alpha F_\pm(0)} \log[1 - N_{\nu_s}^{\text{eff}}]. \quad (70)$$

In fig. 4 we show the curves in the plane  $(s^2, |\delta m^2|)$  that correspond to a constant value  $N_{\nu_s}^{\text{eff}}$  that is proportional to the energy density of the sterile neutrinos at low temperature. It can be seen that the region of parameters that is allowed by the atmospheric neutrino data implies that the sterile neutrinos are fully thermalized (with  $N_{\nu_s}^{\text{eff}}$  very close to 1) and this is possibly incompatible with bounds [8] from primordial nucleosynthesis. We note that this conclusion follows from the assumptions that the asymmetry of the medium is negligibly small and that the oscillations only happen between a sterile and a single active neutrino (and their antiparticles).

Our analytic results improve those from the rough criterium  $\Gamma_{\alpha s}/H(T) \lesssim 1$  [27, 5, 28, 6, 7] and can be compared directly with the numerical results from density matrix approach found in [6, 7] (where momentum-dependence was not included, but it appears from our results that it does not play any role). In the case of interest for us,  $\alpha = \mu, \tau$ , the comparison gives a good agreement. It may be noted that for maximal mixing we have slightly too restrictive results since we neglected the effect of depletion of active neutrino numbers when transitions occur below the chemical decoupling temperature at about 3.5 Mev. For this same reason our results cannot be applied to the case  $\alpha = e$  for  $\delta m^2 < 10^{-5}$ . In this case the depletion effect must be taken into account due to the direct role of electron neutrinos in the neutron-proton interconversion rates and moreover the MSW transition plays a fundamental role.

## 4.2 Non vanishing charge asymmetry

We consider now the case where a non vanishing (constant) asymmetry is present in the medium. In this case the density of sterile neutrinos and anti-neutrinos produced by the oscillations could be generally different, and in turn also the net lepton number of standard neutrinos will not stay constant: it is reasonable to approximate it with a constant if it is varying sufficiently slowly, and in any case the complete, dynamical calculation will be considered in section 5. In fig. 5 we plot the effective number of sterile neutrinos at low temperature as a function of the (constant) asymmetry calculated assuming maximal mixing and for different values of  $|\delta m^2|$ . It can be seen that for sufficient large values of  $L^{(\mu)}$  the contribution of the sterile neutrinos to the energy density begins to drop following a power law  $N_{\nu_s}^{\text{eff}} \propto [L^{(\mu)}]^{-\frac{3}{4}}$ . From the figure we can see that with the oscillation parameters indicated by Super-Kamiokande the contribution of sterile neutrinos to the energy density would be sufficiently small if  $L^{(\mu)} \gtrsim 10^{-4}$ .



It is not difficult to obtain analytically an understanding of the suppression of the oscillations due to the presence of the asymmetry  $L^{(\mu)}$ . For  $s^2 = 1$ , the denominator of the integrand in equation (64) can be rewritten:

$$1 + d_0^2 t^{12} + t^8 [|L^{(\mu)}|/\tilde{L} \pm t^2]^2 \quad (71)$$

where the negative sign applies to the case of neutrinos for  $L^{(\mu)} > 0$ , to antineutrinos for  $L^{(\mu)} < 0$ , and we have defined

$$\tilde{L} = \frac{b_\mu^{\frac{2}{3}}}{a_L} |\delta m^2|^{\frac{1}{3}} y^{\frac{1}{3}}. \quad (72)$$

The results discussed in section 4.1 continue to hold if  $|L^{(\mu)}| \ll \tilde{L}$ ; we consider here the opposite case,  $L^{(\mu)} \gg \tilde{L}$  (or  $-L^{(\mu)} \gg \tilde{L}$ ). In this case the function  $G_{\nu_s(\bar{\nu}_s)}(y, T \rightarrow 0)$  – see equation (64) – receives important contributions from two different regions: one is the region of low temperatures,  $t \sim (L^{(\mu)} / \tilde{L})^{-1/4}$ , another is a high temperature region, where a resonance occurs for  $t = (L^{(\mu)} / \tilde{L})^{1/2}$ . It happens that the first region (low temperature) gives the dominant contribution (and therefore the productions of sterile neutrinos and antineutrinos are similar), and this explains the behavior of the sterile neutrino number with increasing lepton asymmetry, visible in fig. 5, namely

$$G_{\nu_s}^{\text{low}}(y, T \rightarrow 0)|_{s^2=1} \simeq 0.43 (L^{(\mu)} / \tilde{L})^{-3/4}. \quad (73)$$

The resonant high temperature contribution would give instead a behavior

$$G_{\nu_s}^{\text{high}}(y, T \rightarrow 0)|_{s^2=1} \simeq \frac{1}{2 d_0} \left( \frac{L^{(\mu)}}{\tilde{L}} \right)^{-\frac{9}{2}}, \quad (74)$$

that is therefore more suppressed at large  $L^{(\mu)}$ .

Note that for  $s^2 \simeq 1$  the effect of a charge asymmetry of the medium results in a suppression of the sterile neutrino and anti-neutrino population. The situation can be different for  $s^2$  small. In this case the presence of a charge asymmetry can even result in an enhancement of the oscillations. This is illustrated in figs. 6 and 7. In fig. 6 we show a case of enhancement of the sterile production, present for  $\delta m^2 > 0$  and  $s^2 \ll 1$  (a similar behavior was also noticed for much smaller values of  $\delta m^2$  in [29]). For these oscillation parameters, in a neutral medium there is never a situation of maximal mixing, however for a sufficiently large asymmetry neutrinos or antineutrinos with adimensional momentum  $y$  can pass through a resonance for two well defined values of the temperature (see fig. 1). At the lowest  $T$  value the production of sterile neutrinos (or anti-neutrinos) can be significant, and in fact, for positive asymmetry, the production of neutrinos for positive  $\delta m^2$  becomes equal to the production of antineutrinos for negative  $\delta m^2$ , since in both cases we have resonances with almost identical characteristics. In fig. 6 the behavior for large  $L^{(\mu)}/\tilde{L}$  shows a decrease with the same power law as in equation (73).

For still smaller values of  $s^2$ , it is possible to have an intermediate region of asymmetries, still larger than  $\tilde{L}$ , where the sterile neutrino production increases with the

asymmetry. An example of this behavior is given in fig. 7. In fact, integrating with a saddle point approximation for  $L^{(\mu)}/\tilde{L} \gg 1$ , one finds for the resonant component (in the approximation  $c \simeq 1$ ):

$$G(y, T \rightarrow 0) \simeq \frac{\pi}{4} \left( \frac{\tilde{L}}{L^{(\mu)}} \right)^{\frac{3}{4}} \left[ s^2 + d_0^2 \left( \frac{\tilde{L}}{L^{(\mu)}} \right)^3 \right]^{-\frac{1}{2}} \quad (75)$$

Note that for very large  $L^{(\mu)}$  the oscillations are suppressed as before, however for a certain range of values of  $L^{(\mu)}$  determined by the value of  $s^2$  one can have an enhancement.

It should be clear from the arguments given above that the main contributions to the integrals come from rather restricted regions of temperature (particularly if a resonance is present) and therefore the requirement of a constant  $L^{(\mu)}$  for the validity of these results can be slightly relaxed: it is in fact sufficient that the asymmetry is slowly varying in the relevant region of the integration.

## 5 Mixing of two neutrino flavors

In this section we will study the flavor evolution of the neutrino populations in the case of two-flavor mixing of a standard and a sterile neutrino, considering the lepton asymmetry of the medium as a dynamical variable. We will confirm the finding of [23], that for  $\delta m^2 < 0$  one has in general the generation of a large lepton asymmetry  $L_{\nu_\alpha}$ ; at the same time, summing over  $\nu$ 's and  $\bar{\nu}$ 's, the energy density of the sterile neutrinos generated by the oscillations remains similar to what has been obtained in the previous section using the (incorrect) assumption that the charge asymmetry of the medium remains small.

The set of differential equations that we need to solve (31), (32), (33), (34) has been introduced in section 2. In section 3 we have recalled that the collisional operators maintain the active neutrinos in thermal equilibrium, therefore their momentum distributions are determined by the chemical potential  $\xi_\alpha(T) = -\bar{\xi}_\alpha(T)$ , or equivalently (see equation (38)) by the lepton number  $L_{\nu_\alpha}(T)$ . Thus the flavor evolution is described by a set of only two equations, such as (46) and (47) or (51) and (52). We have however to take into account that the lepton number of the medium is evolving with time. The only source of variation of the lepton number is the presence of oscillations, therefore one has that  $L_{\nu_\alpha} + L_{\nu_s}$  remains constant and:

$$L_{\nu_\alpha}(T) + \text{const} = -L_{\nu_s}(T) = \frac{1}{4\zeta(3)} \int dy y^2 [-f_{\nu_s}(y, T) + f_{\bar{\nu}_s}(y, T)]. \quad (76)$$

In summary the problem of the flavor evolution of the neutrino population has been reduced to the solution of the set of two equations (46) and (47), with the additional condition that the asymmetry  $L_{\nu_\alpha}$  that enters in the expression of the transition rates  $\Gamma_{\alpha s}$  and determines the distributions of the standard neutrino and anti-neutrino population is obtained with the integral (76).

It is instructive to consider an equation directly for  $L_{\nu_\alpha}$  that can be obtained combining the definition (76) with equations (46) and (47). The result is:

$$\frac{dL_{\nu_\alpha}}{dt} = \frac{1}{4\zeta(3)} \int dy y^2 f_{eq}^0(y) [(\Gamma_{\alpha s} - \bar{\Gamma}_{\alpha s})(z_s^+ - z_\alpha^+) + (\Gamma_{\alpha s} + \bar{\Gamma}_{\alpha s})(z_s^- - z_\alpha^-)] . \quad (77)$$

This equation allows to understand the evolution of the lepton number making use of some simple considerations. The second term tends to bring the neutrino population toward a situation in which the initial lepton asymmetry is equally shared between active and sterile neutrinos. The first term, for positive  $\delta m^2$ , has always sign opposite to  $L^{(\alpha)}$ , and also acts as a damping term, so that the asymmetry approaches a constant value  $-\tilde{\eta}/2$ , with  $\tilde{\eta} \equiv L^{(\alpha)} - 2L_{\nu_\alpha}$ .

On the other hand, if  $\delta m^2$  is negative, the first term can have either the opposite or the same sign as  $L^{(\alpha)}$  and may also be the source of a growth for the asymmetry. To have an appreciable growth we need that the transition rates for neutrinos and anti-neutrinos are different and that the total number of active neutrinos and sterile neutrinos are also different [30]. Therefore considering the oscillation of two active neutrino species that have approximately equal number densities, one expects only an effect of equipartition of the initial asymmetry. A small effect would arise after chemical decoupling because of a small number density difference between the active neutrinos. This is created by electron-positron annihilations that reheat only the electron neutrino component [31]. Things can be much more interesting in the case of active-sterile neutrino mixing.

In fig. 8 we show as a function of the temperature the energy density of the sterile neutrinos, always calculated assuming the existence of  $\nu_{\mu(\tau)} \leftrightarrow \nu_s$  oscillations with maximal mixing, positive  $\delta m^2 = 3 \times 10^{-3} \text{ eV}^2$  and different initial values of the asymmetry  $L^{(\alpha)}$  ( $0, 10^{-7}, 10^{-6}, 10^{-5}$  and  $10^{-4}$ ). The thin curves show the results of a calculation performed considering  $L^{(\alpha)}$  constant in time: increasing  $L^{(\alpha)}$  the sterile neutrino production is more and more suppressed. The thick lines have been calculated assuming the initial values for the asymmetry, but taking into account the evolution with time of the lepton number. To a good approximation for any initial value  $L^{(\alpha)} \lesssim 10^{-4}$  the initial lepton number is efficiently destroyed and the evolution of the effective number of sterile neutrinos is independent on the initial lepton number and similar to the  $L^{(\alpha)} = 0$  case (three curves are coincident with the thick solid line). For  $L^{(\alpha)} \gtrsim 10^{-4}$  the lepton number remains approximately constant and the results are very similar to the case in which the evolution of the lepton number with temperature is neglected.

In fig. 9 we show the evolution with temperature of the lepton number  $L_{\nu_\alpha}$  ( $\alpha = \mu, \tau$ ) calculated with a numerical integration of the flavor evolution equations, assuming the existence of  $\nu_s \leftrightarrow \nu_{\mu(\tau)}$  oscillations with a negative  $\delta m^2$ , and some representative choices of the mixing angle. The evolution of the neutrino populations is started at  $T = 150 \text{ MeV}$  with  $L_{\text{in}}^{(\alpha)} = 10^{-10}$  and  $\tilde{\eta} = 5 \times 10^{-11}$ .

One can distinguish several phases in the evolution of  $L_{\nu_\alpha}$ : (i) initially the asymmetry  $L^{(\alpha)}$  is erased and  $L_{\nu_\alpha}$  is brought to the value  $-\tilde{\eta}/2$ , (ii) then at a critical temperature  $T_c$  the asymmetry starts an exponential growth, (iii) after a short time the exponential growth is transformed into a power law growth, and (iv) finally the asymmetry is ‘frozen’

and remains at a constant value.

Some insight on the onset of the instability can be obtained with the following qualitative discussion, where we will assume for simplicity that the oscillating flavors are  $\nu_\tau$  and  $\nu_s$ . In this case, as we have discussed in section 2, the resonant momenta for neutrinos and anti-neutrinos are ordered as  $y_{\nu_\tau}^{\text{res}} > y_{\bar{\nu}_\tau}^{\text{res}}$  for  $L^{(\tau)} > 0$  or  $y_{\nu_\tau}^{\text{res}} < y_{\bar{\nu}_\tau}^{\text{res}}$  for  $L^{(\tau)} < 0$  (the values are equal in a neutral medium). Let us now consider the evolution of the asymmetry  $L^{(\tau)}$  with temperature starting from an arbitrary initial value. The values of the resonant momenta, initially very low, increase with time  $y_{\nu_\tau}^{\text{res}} \simeq y_{\bar{\nu}_\tau}^{\text{res}} \simeq \sqrt{c} [T^*(\delta m^2)/T]^3$ . When the resonant values become of order unity the oscillations begin to have effect and start to produce sterile neutrinos and anti-neutrinos. For a certain time, when the position of the resonant momenta is below the peak of the Fermi-Dirac distribution of the standard neutrinos, no lepton asymmetry is produced and in fact any small initial non-zero value of  $L^{(\tau)}$  is erased. This can be easily understood observing that if in this situation (when both resonant values of the adimensional momentum are below the peak of the distribution) a small positive (negative)  $L^{(\tau)}$  develops, the resonance for the neutrinos will move to higher (lower) values of  $y$ , with respect to the position of the resonance for anti-neutrinos; therefore the neutrinos will oscillate more (less) efficiently, and since the sterile particles are much less abundant than the standard ones, this will result in the net disappearance of  $\nu_\tau$ 's ( $\bar{\nu}_\tau$ 's) and in the generation of a negative (positive)  $L_{\nu_\tau}$  that will tend to cancel the initial fluctuation of the charge number  $L^{(\tau)}$ . In summary an initial value of the charge asymmetry will be erased and  $L^{(\tau)}$  will take a value close to zero. This mechanism of destruction of an initial charge asymmetry cannot work if the initial asymmetry is too large and becomes inefficient for  $|L^{(\alpha)}| \gtrsim 10^{-4}$  [32].

The argument outlined above to justify the stability of the condition  $L^{(\tau)} = 0$  obviously loses its validity when the resonant momenta are above the peak of the Fermi-Dirac distribution, at  $y \simeq 2.2$ . More precisely when the temperature drops below a critical value  $T = T_c$  such that

$$y_{\nu_\tau}^{\text{res}} \simeq y_{\bar{\nu}_\tau}^{\text{res}} \simeq \sqrt{c} \left( \frac{T^*}{T_c} \right)^3 \simeq 2.2 \quad (78)$$

the situation becomes unstable. A small positive fluctuation of  $L^{(\tau)}$  results in a larger resonant value for the neutrinos so that the oscillations of the anti-neutrinos become more efficient, more  $\bar{\nu}_\tau$ 's disappear and the asymmetry  $L_{\nu_\tau}$  increases even more. The same argument shows that an initial negative fluctuation in  $L^{(\tau)}$  after  $T_c$ , would grow to a much larger (in absolute value) negative asymmetry.

At first sight it appears that we have a genuine case of instability and that the sign of the lepton number will be determined only by random fluctuations. This is in fact *not* the case, at least in the theoretical framework we are considering. It is possible to demonstrate that asymptotically (for  $T \rightarrow 0$ ) the sign of the lepton asymmetry will be the same as the sign of  $\tilde{\eta} = L_{\nu_e} + L_{\nu_\mu} - B_n/2$ , which is the charge asymmetry of the medium excluding the contributions of the  $\nu_\tau$ 's and that in the present discussion remains constant [11]. Note that it can be expected that  $\tilde{\eta}$  is positive. This can be derived from the assumptions that (i) the electric charge of the universe vanishes ( $L_e = B_p$ ), (ii) the net quantum number  $B - L$  of the universe also vanishes, (iii) protons and neutrons have equal number densities

(for  $T > 3$  MeV) and therefore  $B_p = B_n$ , and (iv) the total lepton number of the standard neutrinos before the development of the oscillations is equally divided among all flavors ( $L_{\nu_e} = L_{\nu_\mu} = L_{\nu_\tau}$ ). From these assumptions one can derive  $\tilde{\eta} = B_p/6$ , that is a positive number of order  $10^{-10}$ . At the critical temperature, where the term proportional to  $L_{\nu_\tau}$  in the right hand side of equation (77) vanishes, and the sterile neutrino asymmetry is still negligible, the sign of the time derivative of  $L_{\nu_\tau}$  is the same as the sign of  $\tilde{\eta}$ ; therefore, once the term driving the instability starts to dominate,  $|L_{\nu_\tau}|$  will continue to grow, and the sign will be the same as the sign of  $\tilde{\eta}$ . We will come back to this point and briefly reconsider the limitations of the present approach in the concluding section.

In fig. 10 and 11 we show the evolution of the distributions of sterile neutrinos and antineutrinos with temperature. We can again distinguish different regimes. In a first phase, for  $T$  larger than a critical temperature  $T_c$ , the initial small asymmetry of the medium is erased, the resonant momentum for neutrinos and anti-neutrinos grows ( $y^{\text{res}} \propto T^{-3}$ ) producing sterile neutrinos with higher and higher momentum. During this phase (as discussed in section 4) the sterile neutrino population, for  $y < y^{\text{res}}(T)$ , is proportional to a thermal distribution, that is  $z_s(y)$  and  $\bar{z}_s(y)$  are constants up to a maximum  $y \lesssim y^{\text{res}}(T)$  (compare with fig. 3).

When the temperature drops below the critical temperature and the production of a positive  $L_{\nu_\tau}$  starts, the resonant momentum for anti-neutrino oscillations is pushed back to lower values producing additional sterile anti-neutrinos. In fig. 10 it appears clearly that the critical temperature corresponds to the situation where the resonant momentum was  $y_{\nu_\tau(\bar{\nu}_\tau)}^{\text{res}} \simeq 2.2$ .

Fig. 11 is calculated for the same value of  $\delta m^2$ , but for a larger mixing parameter  $s^2$ . In this case the critical temperature is lower and corresponds to a situation where the resonant momenta for neutrinos and anti-neutrinos is larger,  $y_{\nu_\tau(\bar{\nu}_\tau)}^{\text{res}} \simeq 7.1$ . An understanding of this “delay” of the onset of the instability for large  $s^2$  can be obtained inspecting equation (77). It can be seen that the term that controls the growth of the asymmetry is  $(\Gamma_{\alpha s} - \bar{\Gamma}_{\alpha s})(z_s^+ - z_\alpha^+)$ . This term is reduced if the sterile neutrinos develop a sizeable population, as it is the case for a sufficiently large  $s^2$ . We can see in fig. 11 that the sterile neutrinos produced in the early phase ( $T > T_c$ ) are in fact a significant fraction of the thermal equilibrium population.

The estimate of the energy density in sterile neutrinos and anti-neutrinos produced by oscillations for  $T \rightarrow 0$ , is modified with respect to the estimates developed in the previous section, because of the effects of the evolution of the lepton asymmetry that determines the neutrino effective potential. It is important to note that the difference between the estimates (with and without the dynamical evolution of  $L_{\nu_\alpha}$ ) is small for those oscillation parameters that predict an appreciable energy density,  $N_{\nu_s}^{\text{eff}} \gtrsim 0.3$ . This is illustrated in fig. 12 where the two thin solid lines in the plane  $(s^2, \delta m^2)$  correspond to  $N_{\nu_s}^{\text{eff}} = 0.1$  and 0.6 in a complete calculation of the flavor evolution, while the two thin dot-dashed lines are calculated assuming a constant negligible  $L_{\nu_\alpha}$ . Note that there is some difference in the results for  $N_{\nu_s}^{\text{eff}} = 0.1$  (so that in the complete calculation the region having  $N_{\nu_s}^{\text{eff}} < 0.1$  is larger), but the two lines corresponding to  $N_{\nu_s}^{\text{eff}} = 0.6$  are essentially indistinguishable. This can be understood qualitatively (see also the discussion in [11, 33]):

when the production of sterile neutrino is sufficiently strong, the lepton number generation is delayed (the critical temperature becomes lower), and the subsequent production of sterile neutrinos in the regime with a not negligible lepton number occurs far from the peak of the Fermi distribution, and therefore gives a small contribution, see fig. 11.

Thus we can conclude that in the simplest framework of two-flavor active-sterile neutrino mixing a detailed treatment of the lepton number generation does not essentially modify the region of oscillation parameters that the constraints of BBN can exclude. As we will discuss in the next section, this is not true any more if we consider a more general framework with more elaborate forms of mixing between neutrino flavors.

## 6 Three neutrinos mixing scenario

In this section we will consider the scenario proposed by Foot and Volkas [11] where a sterile neutrino is mixed with both  $\nu_\mu$  and  $\nu_\tau$ . As in [11] we will not consider the most general case of three neutrino mixing but we will limit our considerations to a situation where we can neglect the  $\nu_\mu \leftrightarrow \nu_\tau$  oscillations and the descriptions of all transitions can be well approximated by a pair of two-flavor oscillations:  $\nu_\mu \leftrightarrow \nu_s$  and  $\nu_\tau \leftrightarrow \nu_s$ . In the scenario we are considering two neutrino eigenstates are nearly degenerate with a squared mass difference of order  $\delta m_\mu^2 \sim 3 \times 10^{-3} \text{ eV}^2$ , and are both superpositions with approximately equal weights of  $\nu_\mu$  and  $\nu_s$  and only a small component of  $\nu_\tau$ ; in this way the  $\nu_\mu \leftrightarrow \nu_s$  oscillations can describe the atmospheric neutrino data. The third mass eigenstate is nearly a pure  $\nu_\tau$ .

As we have seen before, if the  $\nu_\tau$  does not participate in the oscillations, the  $\nu_\mu \leftrightarrow \nu_s$  transitions result in an energy density in sterile neutrinos not compatible with suggested bounds from big bang nucleosynthesis, unless an unnaturally high lepton number  $L^{(\mu)}$  is present at the start and persists down to temperatures  $T \lesssim 10 \text{ MeV}$ . The inclusion of a small mixing of the  $\tau$  neutrinos deeply modifies this conclusion. The oscillations between  $\nu_\tau$  and  $\nu_s$  can produce a significant  $L_{\nu_\tau}$  and this in turn can suppress the production of sterile neutrinos in the  $\nu_\mu \leftrightarrow \nu_s$  oscillations.

For this mechanism to work it is necessary to require  $|\delta m_\tau^2| \geq |\delta m_\mu^2|$  (so that the  $\nu_\tau \leftrightarrow \nu_s$  oscillations start earlier),  $\delta m_\tau^2 < 0$  (the mass eigenstate dominantly coupled to  $\nu_\tau$  is the heaviest) and  $s_\tau^2$  sufficiently small (to assure that the lepton number generation can actually occur). Moreover the constraint (70) must be verified, otherwise a sterile neutrino overproduction would occur already during the early  $\nu_\tau \leftrightarrow \nu_s$  oscillations. These conditions are not sufficient by themselves to prevent a subsequent destruction of the lepton number by the  $\nu_\mu \leftrightarrow \nu_s$  oscillations and as a consequence  $N_{\nu_s}^{\text{eff}} \simeq 1$ . In the following the conditions on the oscillation parameters to avoid this conclusion are discussed.

We indicate with  $s_\alpha$ ,  $c_\alpha$ ,  $\delta m_\alpha^2$  ( $\alpha = \mu, \tau$ ) the mixing parameters for the  $\nu_\alpha \leftrightarrow \nu_s$  oscillations. The set of equations that describe the flavor evolution for the proposed scenario can be easily obtained with a simple generalization of the case of two flavor mixing discussed in section 5, describing at the same time the dynamical evolution of the two lepton numbers  $L_{\nu_\mu}$  and  $L_{\nu_\tau}$ . As before the active (anti-)neutrinos are assumed

to be in thermal equilibrium, namely, neglecting terms of second order in the chemical potential,  $z_\mu^+ = z_\tau^+ \simeq 1$ ,  $z_{\mu(\tau)}^- \simeq 12 \zeta(3) L_{\nu_{\mu(\tau)}} / [\pi^2 (1 + e^{-y})]$ . Thus we can write:

$$\frac{dL_{\nu_\tau}}{dt} = -\frac{1}{4\zeta(3)} \int dy y^2 f_{eq}^0(y) \{[\Gamma_{\tau s} - \bar{\Gamma}_{\tau s}] (1 - z_s^+) + [\Gamma_{\tau s} + \bar{\Gamma}_{\tau s}] (z_\tau^- - z_s^-)\} \quad (79)$$

$$\frac{dL_{\nu_\mu}}{dt} = -\frac{1}{4\zeta(3)} \int dy y^2 f_{eq}^0(y) \{[\Gamma_{\mu s} - \bar{\Gamma}_{\mu s}] (1 - z_s^+) + [\Gamma_{\mu s} + \bar{\Gamma}_{\mu s}] (z_\mu^- - z_s^-)\} \quad (80)$$

$$\frac{d}{dt} z_s(y, t) = [\Gamma_{\tau s} + \Gamma_{\mu s}] [1 - z_s(y, t)] \quad (81)$$

$$\frac{d}{dt} \bar{z}_s(y, t) = [\bar{\Gamma}_{\tau s} + \bar{\Gamma}_{\mu s}] [1 - \bar{z}_s(y, t)] \quad (82)$$

Note that the evolutions of the two asymmetries  $L_{\nu_\mu}$  and  $L_{\nu_\tau}$  are coupled for two reasons, the first being simply that  $\nu_s$  oscillate both in  $\nu_\mu$  and in  $\nu_\tau$ , the second is that, also when the population of sterile neutrinos is small and the transitions  $\nu_s \rightarrow \nu_{\mu(\tau)}$  can be neglected, the asymmetry of one type of flavor (for example  $L_{\nu_\tau}$ ) is relevant for the evolution of the other asymmetry (in this case  $L_{\nu_\mu}$ ) because it modifies the effective potential in the medium of the neutrino ( $\nu_\mu$ ).

We have numerically integrated this set of equations calculating as a function of temperature the distributions of sterile neutrinos and the asymmetries of  $\nu_\mu$ 's and  $\nu_\tau$ 's. The results show some very interesting and not entirely intuitive features. In fig. 12 we show curves of constant energy density in sterile neutrinos for  $T \rightarrow 0$  as a function of the oscillation parameters  $\delta m_\tau^2$  and  $s_\tau^2$  assuming  $s_\mu^2 = 1$  and a fixed value of  $\delta m_\mu^2$ . The most remarkable feature is that for a given value of  $\delta m_\mu^2$  the plane ( $s_\tau^2, \delta m_\tau^2$ ) is divided in two regions. In one (the region below the thick lines) the sterile neutrinos become fully thermalized, while in the other (above these lines) the energy density in sterile neutrinos drops to a much lower value. This value is almost undistinguishable from what is obtained in a calculation with only  $\nu_\tau \leftrightarrow \nu_s$  oscillations (the  $\nu_\mu \leftrightarrow \nu_s$  oscillations being completely damped). In fact, the lines of constant  $N_{\nu_s}^{\text{eff}}$  in fig. 12 drawn as thin lines are exactly the same that were obtained and discussed in section 5 using a two-neutrino scenario.

The boundary in parameter space between the region where the sterile neutrino is thermalized (resulting in  $N_{\nu_s}^{\text{eff}} \simeq 1$ ) and the region where the effect of  $\nu_\mu \leftrightarrow \nu_s$  oscillations is essentially negligible is given to a first approximation by the relation

$$s_\tau^2 (\delta m_\tau^2)^2 \simeq 28 (\delta m_\mu^2)^2 \quad (83)$$

(see the dashed curves in fig. 12). From the figure, we read that the minimum value allowed for the tau-neutrino mass in order to comply the BBN bounds is  $\sim 1.4$  eV (3 eV) if  $\delta m_\mu^2 = 10^{-3}$  ( $3.2 \times 10^{-3}$ ) eV<sup>2</sup>, with a mixing angle  $s_\tau^2 \simeq 10^{-5}$ .

In fig. 13 we show the evolution with temperature of the sterile neutrino effective number considering values for the neutrino oscillation parameters that are very close to each other but belong to the two different regions where the sterile neutrinos are or are not thermalized. The thick lines correspond to a point immediately below the corresponding

boundary in fig. 12: the sterile neutrino production is momentarily interrupted when the  $\nu_\tau$  asymmetry is generated at a temperature of about 30 MeV, but, since the initial rapid increase of  $L^{(\mu)}$  is stopped and then reversed, it starts again and reaches the thermal equilibrium at a temperature  $\sim 10$  MeV. The thin lines, corresponding to a point immediately above the boundary in fig. 12, describe a situation in which  $L^{(\mu)}$  continues to increase, and the  $\nu_\mu \leftrightarrow \nu_s$  oscillations are damped and unable to generate further sterile neutrinos.

In the following we will present some qualitative arguments and analytic estimates to illustrate these numerical results.

## 6.1 Qualitative discussion

In fig. 14 we show an illustration of the neutrino mixing parameters in matter at different times (or temperatures). This particular example was calculated for the set of oscillation parameters:  $\delta m_\mu^2 = 10^{-3} \text{ eV}^2$ ,  $s_\mu^2 = 1$ ,  $\delta m_\tau^2 = -10 \text{ eV}^2$ ,  $s_\tau^2 = 10^{-6}$ . In each panel the four different curves describe the effective mixing parameter for the four transitions between standard and sterile (anti-)neutrinos:  $s_{\mu,m}^2$ ,  $\bar{s}_{\mu,m}^2$ ,  $s_{\tau,m}^2$ , and  $\bar{s}_{\tau,m}^2$ ; the different panels refer to different temperatures, from top to bottom the temperatures and asymmetries in the five panels correspond to the situations (a) :  $T = 58.1 \text{ MeV}$ ,  $L_{\nu_\tau} = 0$ , (b) :  $T = 38.7 \text{ MeV}$ ,  $L_{\nu_\tau} = 0$ , (c) :  $T = 34.9 \text{ MeV}$ ,  $L_{\nu_\tau} = 8.9 \times 10^{-7}$ , (d) :  $T = 32.2 \text{ MeV}$ ,  $L_{\nu_\tau} = 1.7 \times 10^{-6}$ , (e) :  $T = 29.1 \text{ MeV}$ ,  $L_{\nu_\tau} = 3.2 \times 10^{-6}$  and in all cases  $L_{\nu_\mu} \simeq 0$ . The behaviour of the evolution of the mixing parameters is easy to understand qualitatively. At high temperatures the medium is neutral and the oscillation parameters in matter for  $\nu$ 's and  $\bar{\nu}$ 's are equal. For vanishing charge asymmetry of the medium, the mixing parameter in matter for  $\nu_\mu \leftrightarrow \nu_s$  oscillations is

$$s_{\mu,m}^2 = \bar{s}_{\mu,m}^2 = \left[ 1 + \left( \frac{b_\mu T^6 y^2}{\delta m_\mu^2} \right)^2 \right]^{-1} \simeq \left( \frac{T_\mu^*}{T} \right)^{12} y^{-4} \quad (84)$$

and the mixing is strongly suppressed by matter effects. For the  $\nu_\tau \leftrightarrow \nu_s$  oscillations, the important feature is the fact that at a momentum

$$y_{\nu_\tau}^{\text{res}} = y_{\bar{\nu}_\tau}^{\text{res}} = \sqrt{c_\tau} \left( \frac{\delta m_\tau^2}{b_\tau} \right)^{\frac{1}{2}} T^{-3} = \sqrt{c_\tau} \left( \frac{T_\tau^*}{T} \right)^3 \quad (85)$$

the mixing for neutrinos and antineutrinos is maximal. With decreasing temperature the suppression of the  $\nu_\mu \leftrightarrow \nu_s$  oscillations becomes weaker while the position of the resonance for the  $\nu_\tau \leftrightarrow \nu_s$  oscillations grows as  $T^{-3}$ . When  $y_{\nu_\tau}^{\text{res}}$  approaches the peak of the Fermi distribution, the instability discussed previously sets in and an asymmetry  $L_{\nu_\tau}$  becomes to develop. The positions of the resonances for the tau-sterile oscillations of neutrinos and anti-neutrinos are given by equation (15) for  $\alpha=\tau$ . If a positive  $L_{\nu_\tau}$  starts to be generated the resonance for the neutrinos moves to higher momenta  $y$ , where the neutrino population is smaller, therefore  $\bar{\nu}_\tau$  oscillate more effectively, and the asymmetry grows faster.

An important consequence of the generated  $L_{\nu_\tau}$  is to modify the oscillation parameters of the  $\nu_\mu \leftrightarrow \nu_s$  oscillations. The presence of an  $L^{(\mu)}$  asymmetry depresses the oscillations



for most values of the neutrino momentum, but also induces maximal mixing for neutrinos or antineutrinos (depending on the sign of  $L^{(\mu)}$ ) in a narrow range of momenta. For positive  $L^{(\mu)} \simeq L_{\nu_\tau}$  the resonance is present for neutrinos at a momentum

$$y_{\nu_\mu}^{\text{res}} = \frac{a_L}{b_\mu} \frac{L^{(\mu)}}{T^2} \quad (86)$$

and it gives rise to the generation of a negative  $L_{\nu_\mu}$ , that also acts on the oscillation parameters for both type of oscillations.

It appears clearly now that two different scenarios can develop. In the first case the generation of  $L_{\nu_\mu}$  is never sufficiently rapid to cancel the growth of  $L_{\nu_\tau}$ , and the combined asymmetry  $L^{(\mu)} \simeq 2L_{\nu_\mu} + L_{\nu_\tau}$  keeps growing. The resonant peak for the muon neutrino oscillations rapidly ( $y_{\nu_\mu}^{\text{res}} \propto L^{(\mu)}/T^2$ ) moves to very high values of  $y$  where it becomes irrelevant because no neutrinos have such a high momentum, and the  $\nu_\mu \leftrightarrow \nu_s$  oscillations remain suppressed by the generated  $L^{(\mu)}$  (this is the situation envisaged in fig. 14). In the second possible outcome, the oscillations  $\nu_\mu \leftrightarrow \nu_s$  proceed so rapidly that at a certain time the growth of  $L^{(\mu)}$  is stopped and then reversed. Qualitatively it is understandable that in the space of oscillation parameters there will be a sharp boundary between regions where the two different scenarios develop. For example let us keep fixed  $\delta m_\mu^2$ ,  $\delta m_\tau^2$  and  $s_\mu^2 = 1$ , and consider the evolution of the neutrino populations for different  $s_\tau^2$ . In a certain interval of  $s_\tau^2$  the oscillations of tau–neutrinos proceed sufficiently rapidly to generate a net  $L^{(\mu)}$  and suppress the muon–neutrino oscillations. Decreasing  $s_\tau^2$  the rates for the  $\nu_\tau \leftrightarrow \nu_s$  transitions, equations (35, 36), become weaker and weaker and the generation of  $L_{\nu_\tau}$  slower. At a critical value the  $\bar{\nu}_\tau \leftrightarrow \bar{\nu}_s$  oscillations do not proceed sufficiently rapidly to cancel the effect of the  $\nu_\mu \leftrightarrow \nu_s$  oscillations and the growth of  $L^{(\mu)}$  can be stopped and reversed.

Qualitatively it should be clear that for a set of parameters along the boundary between the two regions the conditions (temperature and asymmetries of the medium) when the derivative  $dL^{(\mu)}/dt$  vanishes and the growth of the asymmetry is reversed are such that the resonance for the  $\nu_\mu \rightarrow \nu_s$  transitions is close to the maximum of the Fermi distribution ( $y_{\nu_\mu}^{\text{res}} \simeq y_{\text{peak}} = 2.2$ ), where it affects the largest possible neutrino population.

## 6.2 Analytic estimate

To obtain an estimate of the boundary that separates the regions in the space of the neutrino oscillation parameters where the sterile neutrino production is suppressed, we will make the assumption that the reversal of the asymmetry  $L^{(\mu)}$  happens when both the resonances for  $\nu_\mu \leftrightarrow \nu_s$  and  $\bar{\nu}_\tau \leftrightarrow \bar{\nu}_s$  oscillations, that are the source of a negative  $dL_{\nu_\mu}$  and a positive  $dL_{\nu_\tau}$  are most effective, that is in conditions where both resonances are at a value  $y \simeq y_{\text{peak}} \simeq 2.2$  (this corresponds to the situation of panel (d) in fig. 14). We will therefore impose the condition:

$$\left[ 2 \frac{dL_{\nu_\mu}}{dt} + \frac{dL_{\nu_\tau}}{dt} \right]_{y_{\nu_\mu}^{\text{res}} = y_{\bar{\nu}_\tau}^{\text{res}} = y_{\text{peak}}} = 0 \quad (87)$$

This algorithm is motivated by our numerical results that indicate that the reversal happens for values of the temperature and the asymmetries  $L_{\nu_\mu}$  and  $L_{\nu_\tau}$  such that this condition is approximately satisfied. The algorithm can also be understood qualitatively observing that if there is no reversal of the asymmetry  $L^{(\mu)}$  the resonance momentum  $y_{\nu_\mu}^{\text{res}}$  takes all values from zero to infinity and therefore it will take the value  $y_{\text{peak}}$ ; the effect of the  $\nu_\mu \leftrightarrow \nu_s$  oscillations (relative to the  $\bar{\nu}_\tau \leftrightarrow \bar{\nu}_s$  oscillations) is on the other hand most important when  $y_{\nu_\mu}^{\text{res}} \simeq y_{\text{peak}}$ . During the early phase of the generation of  $L_{\nu_\tau}$  one also has  $y_{\bar{\nu}_\tau}^{\text{res}} \lesssim y_{\text{peak}}$ , at least for sufficiently small  $s_\tau^2$  (as illustrated in an example in fig. 10).

The expressions for the derivatives of the lepton asymmetries can be approximated, keeping only the dominant terms, in the following form:

$$\frac{dL_{\nu_\tau}}{dt} \simeq -\frac{1}{4\zeta(3)} \int dy y^2 f_{\text{eq}}^0(y) [\Gamma_{\tau s} - \bar{\Gamma}_{\tau s}] \quad (88)$$

$$\frac{dL_{\nu_\mu}}{dt} \simeq -\frac{1}{4\zeta(3)} \int dy y^2 f_{\text{eq}}^0(y) [\Gamma_{\mu s} - \bar{\Gamma}_{\mu s}] \quad (89)$$

Neglecting furthermore the oscillations of  $\bar{\nu}_\mu$ 's that are non resonant and the oscillations of the  $\nu_\tau$ 's that are happening at large values of  $y$ , and calculating the integrals with the saddle point approximation since they are dominated by the resonance contributions, equation (87) can be rewritten as:

$$\begin{aligned} & -2 \left[ \left( 1 + \frac{(G_F^2 k_\mu)^2 T^{12} y_{\text{peak}}^4}{|\delta m_\mu^2|^2} \right)^{\frac{1}{2}} \left( y_{\text{peak}} \frac{b_\mu T^6}{|\delta m_\mu^2|} \right) \right]^{-1} \\ & + s_\tau^2 \left[ \left( s_\tau^2 + \frac{(G_F^2 k_\tau)^2 T^{12} y_{\text{peak}}^4}{|\delta m_\tau^2|^2} \right)^{\frac{1}{2}} \left( y_{\text{peak}} \left( 2 + \frac{L^{(\tau)}}{L^{(\mu)}} \right) \frac{b_\tau T^6}{|\delta m_\tau^2|} \right) \right]^{-1} = 0 \quad (90) \end{aligned}$$

For  $(G_F^2 k_\tau)^2 T^{12} y_{\text{peak}}^4 / |\delta m_\tau^2|^2 \gg s^2$  and  $(G_F^2 k_\mu)^2 T^{12} y_{\text{peak}}^4 / |\delta m_\mu^2|^2 \gg 1$  the dependence on  $y_{\text{peak}}$  drops away (showing that the choice of that particular value was not critical) and the condition for the boundary takes the simple form

$$s_\tau^2 |\delta m_\tau^2|^2 \simeq 2 \left( 2 + \frac{L^{(\tau)}}{L^{(\mu)}} \right) |\delta m_\mu^2|^2. \quad (91)$$

In this way we have reproduced the functional form ( $s_\tau^2 |\delta m_\tau^2|^2 \simeq \text{const} |\delta m_\mu^2|^2$ ) of the boundary between the regions in parameter space where the  $\nu_\mu \leftrightarrow \nu_s$  oscillations develop or not (see fig. 12). The numerical results can be fitted with the constant approximately equal to 28, and with the analytic estimate sketched above we obtain a reasonable approximation for it. In fact, neglecting the small term  $L_{\nu_e} - B_p/2$ , one has:  $L^{(\tau)} = 2L_{\nu_\tau} + L_{\nu_\mu}$  and  $L^{(\mu)} = 2L_{\nu_\mu} + L_{\nu_\tau}$ ; since  $L_{\nu_\mu}$  is negative we have  $L^{(\tau)}/L^{(\mu)} \geq 2$ .

It is also possible to understand why the thick lines in fig. 12 are not straight for relatively large  $s^2$ , and bend upwards. This is due to the fact that in this situation the resonant momentum  $y_{\bar{\nu}_\tau}^{\text{res}}$  at the critical temperature is larger than  $y_{\text{peak}}$ , and therefore the

approximation of equal  $y_{\nu_\mu}^{\text{res}}$  and  $y_{\bar{\nu}_\tau}^{\text{res}}$  fails. The constraint becomes more restrictive because the tau–sterile antineutrino oscillations are less effective, and a larger  $\delta m_\tau^2$  is needed to compensate this effect.

It is appropriate at this point to comment again on the validity of the approximation implicit in the use of the Pauli–Boltzmann approach, equations (79), (80), (81), (82). It may appear in fact that the use of such an approach for the  $\nu_\mu \leftrightarrow \nu_s$  oscillations is not justified, since  $s_\mu^2 \simeq 1$ . As discussed in section 3, the largest discrepancy from the more accurate treatment based on QKE is to be expected for  $L_{\nu_\mu}$ , determined through equation (80). We note that the only important effect of  $L_{\nu_\mu}$  is to stop and reverse the increase of  $L^{(\mu)}$ , if it succeeds in doing so (otherwise it is always small and ineffective). The inversion, if present, happens when the  $\nu_\mu$  oscillations are resonance dominated, and therefore the condition of validity for the approach is given by equation (41). It is not difficult to verify that this constraint is satisfied for values of  $y$  larger than a lower limit, that on the thick curves in figure 12 is not larger than 0.25: from figure 13 it is apparent that the inversion occurs for considerably larger values of  $y_{\nu_\mu}^{\text{res}}$ . Once  $L^{(\mu)}$  starts to decrease, the detailed behavior of  $L_{\nu_\mu}$  (that might be inaccurately described in our approach) becomes irrelevant, since the sterile neutrinos are abundantly produced anyhow. A confirmation of this comes from the substantial agreement of our results with those obtained using the complete Quantum Kinetic Equations in [25].

## 7 Discussion of the results and conclusions

Our results are in good agreement with the numerical results obtained in [11, 25], except in the region of the highest acceptable  $s_\tau^2$ . The curves of [11], calculated in a Pauli–Boltzmann approach, do not show an upper bending as ours do, while the results obtained in [25] using QKE are slightly more restrictive than our curves.

Our results do not agree with the semi-analytical calculations presented in [34, 35], that obtain a much more stringent lower limit on the tau–neutrino mass ( $m_{\nu_\tau} \gtrsim 15$  eV), that would give too much energy density in the form of hot dark matter and problems for early structure formations. The authors of [34, 35] claim that very small values of  $y_{\nu_\mu}^{\text{res}}$  are most important to determine the fate of the lepton number and that an insufficient resolution in the momenta may well miss this contribution and thus yield wrong results. We have accurately tested our numerical results; for example, the curves in figure 13 describing the behaviour of the asymmetry  $L^{(\mu)}$  remain the same, if we change the minimal value of  $y$  used to calculate the sterile neutrino distribution down to  $10^{-6}$ . This strengthens our result, that the values of  $y_{\nu_\mu}^{\text{res}}$  that can better destroy the lepton number are around  $y_{\text{peak}}$  and not the small ones. We performed the same test in several points in parameter space, that essentially cover the thick curves in figure 12. Moreover we note that for small values of  $y_{\nu_\mu}^{\text{res}}$  (more precisely, for  $y_{\nu_\mu}^{\text{res}} < y_{\bar{\nu}_\tau}^{\text{res}} \sqrt{|\delta m_\mu^2|/|\delta m_\tau^2|} \simeq 10^{-3} - 10^{-2}$  according to the region of parameters considered), the sterile neutrino production from  $\nu_\mu - \nu_s$  transitions has a dominant non–resonant behaviour (and cannot therefore be evaluated in the resonant approximation), which is rather smooth and does not require a resolution particularly

high to be estimated correctly.

Furthermore, we do not agree with the condition imposed in [34, 35] to determine the range of parameters that allow the survival of the lepton number generated. In those papers the amount of lepton number destroyed by  $\nu_\mu \leftrightarrow \nu_s$  oscillations for any  $y_{\nu_\mu}^{\text{res}}$  during the time needed to cross the resonance is compared with the total value of the lepton number  $L^{(\mu)}$  produced up to that moment. In our opinion, the comparison should be done instead with the amount of lepton number created by  $\nu_\tau \leftrightarrow \nu_s$  oscillations during the same time interval (i.e. making a comparison of the two rates as we did). Actually this amount is comparable with the total lepton number created before and in fact it is even more, since the lepton number is exponentially growing.

The same authors have also recently found another argument that should restrict the allowed region [36]. The QKE show a chaotic behaviour for the sign of the lepton number that is generated at the critical temperature [22, 37] and this would lead to the formation of lepton domains. Neutrino crossing the borders of these domains would pass through a further resonance, with an additive contribution to sterile neutrino production. We think that even though on qualitative grounds this observation sets forth an important issue, from a quantitative point of view only a full momentum dependent approach can give a definitive answer about the chaotic behaviour (moreover, the present results of momentum independent calculations [36, 37] are not in good agreement with each other). In [25] such an approach is used and the chaotic behaviour has also been found, but only for large enough mixing angles. A complete analysis of the region in parameter space where chaos occurs is still missing however, and we think that the effect of lepton domain formation on the allowed region may be more accurately determined.

In conclusion, a momentum dependent Pauli-Boltzmann approach for active-sterile neutrino oscillations in the Early Universe allows to derive, directly from the equations, useful analytical results for the sterile neutrino production that support the numerical ones. An analytical procedure provides a deeper physical insight and allows a more general picture of the possible solutions that sometimes pure numerical calculations hide (the generation of a relevant lepton number missed in early numerical results is a good example). In this way we have been able to derive analytically in section 4 the constraints from BBN on mixing parameters with the assumption of negligible lepton numbers, showing that they essentially reproduce the results that can be obtained from QKE for  $\nu_{\mu(\tau)} \leftrightarrow \nu_s$  oscillations. When lepton numbers are present their effect is for most cases a suppression of sterile neutrino production, but we showed that it exists a regime where an enhancement is possible, even if in a parameter region not interesting for the present BBN bound. We were also able to give a full spectral description of the production, both in the case of negligible lepton numbers and when lepton numbers must be considered. This allowed to specify better why in the case of a two neutrino mixing the regions allowed by BBN do not change significantly with or without a generation of lepton number. The most important result has been obtained about the possibility that the generation of lepton number through tau-sterile neutrino oscillations can suppress sterile neutrino production from mu-sterile oscillations for the values of mixing parameters that could describe the Super-Kamiokande results. We confirmed numerically previous results [11], that show

that this is possible with a lower limit on the tau neutrino mass (of a few eV) compatible with present cosmological observations. We could provide an analytical support to these results and show that one should not worry to obtain an exceedingly high resolution in momentum space. This settles in our opinion the recent controversy on the minimum  $\nu_\tau$  mass allowed.

We did not consider the more general situation where lepton domains can be created. We think that clear results about this issue are necessary, but still missing. Anyway it is surely important to have established results in the simpler homogeneous case.

### **Acknowledgments**

We would like to thank E.Kh. Akhmedov, R. Foot and R.R. Volkas for useful discussions.

## References

- [1] Super-Kamiokande collaboration, Y. Fukuda *et al.*, Phys.Rev.Lett. 81, 1562 (1998); K. Scholberg (for the SK collaboration), hep-ex/9905016.
- [2] Kamiokande collaboration, Y. Fukuda *et al.*, Phys. Lett. B 335, 237 (1994); IMB collaboration, R. Becker-Szendy *et al.*, Phys. Rev. D 46, 3720 (1992); Soudan 2 Collaboration, W.W.M. Allison *et al.*, Phys.Lett. B 449, 137 (1999); MACRO collaboration, M. Ambrosio *et al.*, Phys.Lett. B 434, 451 (1998); F. Ronga (for the MACRO collaboration), hep-ex/9810008.
- [3] See for example J.N. Bahcall, P.I. Krastev and A.Yu. Smirnov, Phys.Rev. D 58, 096016 (1998) and references therein.
- [4] LSND Collaboration, C. Athanassopoulos *et al.*, Phys.Rev. C 54, 2685 (1996); Phys.Rev.Lett. 81, 1774 (1998); Phys. Rev. C 58, 2489, (1998).
- [5] R. Barbieri and A.D. Dolgov, Phys.Lett. B 237, 464 (1990); Nucl.Phys. B 349, 743 (1991).
- [6] K. Enqvist, K. Kainulainen and M.J. Thomson, Nucl.Phys. B 373, 498 (1992).
- [7] X. Shi, D.N. Schramm and B.D. Fields, Phys.Rev. D 48, 2568 (1993).
- [8] K.A. Olive, G. Steigman and T.P. Walker, astro-ph/9905320, to be published in Physics Reports (1999).
- [9] E. Lisi, S. Sarkar and F.L. Villante, Phys.Rev. D 59, 123520 (1999).
- [10] D. Kirkman, D. Tytler, S. Burles, D. Lubin and J.M. O'Meara, astro-ph/9907128, and references therein.
- [11] R. Foot and R.R. Volkas, Phys.Rev. D 55, 5147 (1997).
- [12] L. Wolfenstein, Phys.Rev. D 17, 2369 (1978).
- [13] S.P. Mikheyev and A.Yu. Smirnov, Nuovo Cimento C 9, 1 (1986).
- [14] D. Notzold and G. Raffelt, Nucl. Phys. B 307, 924 (1988).
- [15] K. Enqvist, K. Kainulainen and J. Maalampi, Nucl.Phys. B 349, 754 (1991).
- [16] A.D. Dolgov, Sov.J.Nucl.Phys. 33, 700 (1981).
- [17] R.A. Harris and L. Stodolsky, Phys.Lett. B 116, 464 (1982).
- [18] L. Stodolsky, Phys.Rev. D 36, 2273 (1987).
- [19] B.H.J. McKellar and M.J. Thomson, Phys.Rev. D 49, 2710 (1994).

- [20] J. Bernstein, “Kinetic Theory in the Expanding Universe”, Cambridge University Press, Cambridge, 1988.
- [21] N.F. Bell, R.R. Volkas and Y.Y.Y. Wong, Phys.Rev. D 59, 113001 (1999).
- [22] X. Shi, Phys.Rev. D 54, 2753 (1996).
- [23] R. Foot, M.J. Thomson and R.R. Volkas, Phys.Rev. D 53, 5349 (1996).
- [24] R. Foot and R.R. Volkas, Phys.Rev. D 56, 6653 (1997).
- [25] R. Foot, Astropart.Phys. 10, 253 (1999).
- [26] J.M. Cline, Phys.Rev.Lett. 68, 3137 (1992).
- [27] D. Fargion and M.G. Shepkin, Phys.Lett. B 146, 46 (1984).
- [28] K. Kainulainen, Phys.Lett. B 244, 191 (1990).
- [29] D.P. Kirilova and M.V. Chizhov, Nucl.Phys. B 534, 447 (1998).
- [30] M.Yu. Khlopov and S.T. Petcov, Phys.Lett. B 99, 117 (1981); Erratum: Phys.Lett. B 100, 520 (1981).
- [31] P. Langacker, S.T. Petcov, G. Steigman and S. Toshev, Nucl.Phys. B 282, 589 (1987).
- [32] R. Foot and R.R. Volkas, Phys.Rev.Lett. 75, 4350 (1995).
- [33] R. Foot and R.R. Volkas, Astrop.Phys. 7, 283 (1997).
- [34] X. Shi and G.M. Fuller, Phys.Rev. D 59, 063006 (1999).
- [35] X. Shi and G.M. Fuller, astro-ph/9812232.
- [36] X. Shi and G.M. Fuller, astro-ph/9904041.
- [37] K. Enqvist, K. Kainulainen and A. Sorri, hep-ph/9906452.

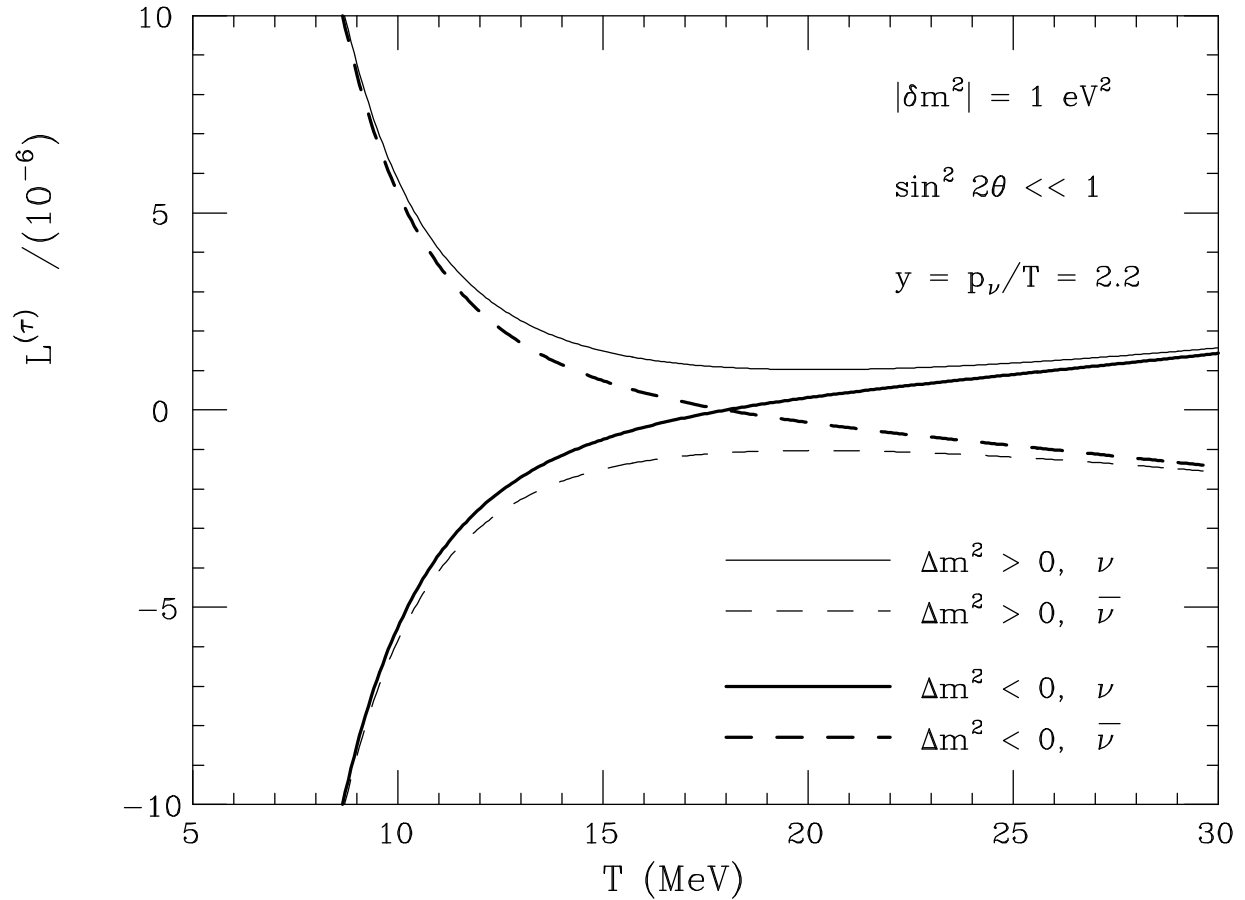


Figure 1: Curves in the plane  $(T, L^{(\alpha)})$  that correspond to maximal mixing for neutrino and anti-neutrinos with  $y = p/T = 2.2$ . All lines are calculated for  $|\delta m^2| = 1 \text{ eV}^2$  and  $s^2 \ll 1$ .



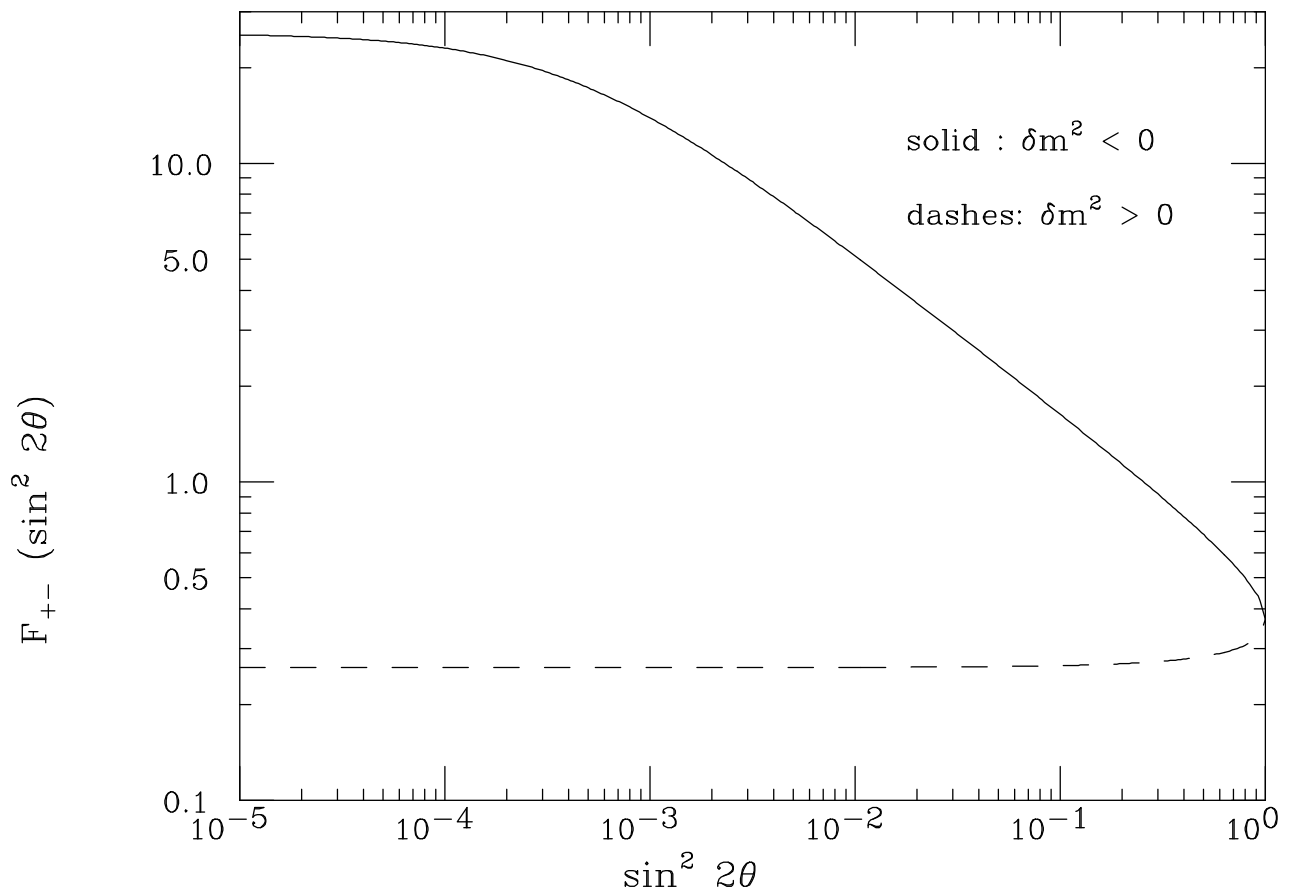


Figure 2: Plot of the functions  $F_+(s^2)$  (dashed line) and  $F_-(s^2)$  (solid line) as a function of the mixing parameter.

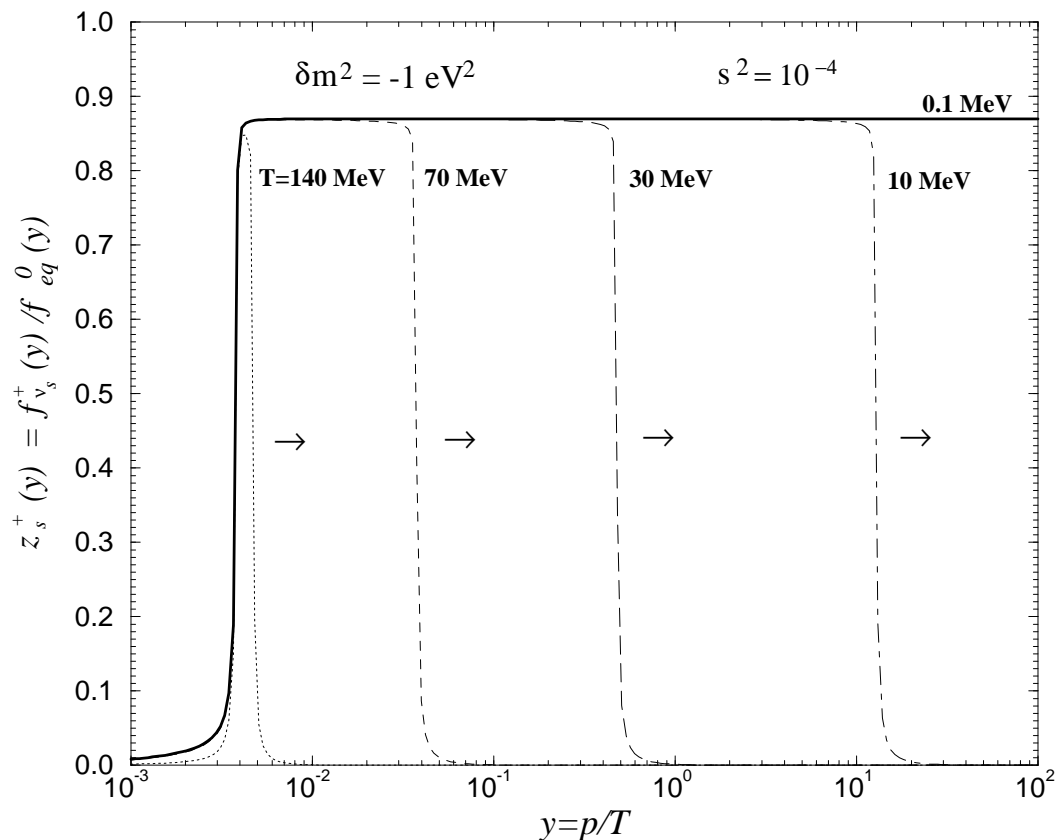


Figure 3: Evolution of the sterile neutrino distribution assuming the presence of  $\nu_s \leftrightarrow \nu_{\mu(\tau)}$  oscillations with  $\delta m^2 = -1 \text{ eV}^2$  and  $s^2 = 10^{-4}$ . The flavor evolution is followed from an initial temperature  $T_i = 150 \text{ MeV}$ , where we assumed that sterile neutrinos are absent. We plot the ratio of momentum distribution of  $\nu_s$ 's and  $\bar{\nu}_s$ 's (equal in this case) with a thermal equilibrium distribution with zero chemical potential. The thick solid line shows the distribution at  $T = 0.1 \text{ MeV}$ , the thin dot-dashed, long-dashed and dashed lines show the distributions for higher values of  $T$ . At each temperature the production of  $\nu_s$  occurs only in a small interval of momenta where oscillations are resonant. As an illustration the dotted curve shows the region where sterile neutrinos are produced for  $T$  just below  $150 \text{ MeV}$ . The direction of the arrows indicates how the resonant momentum is changing with time.

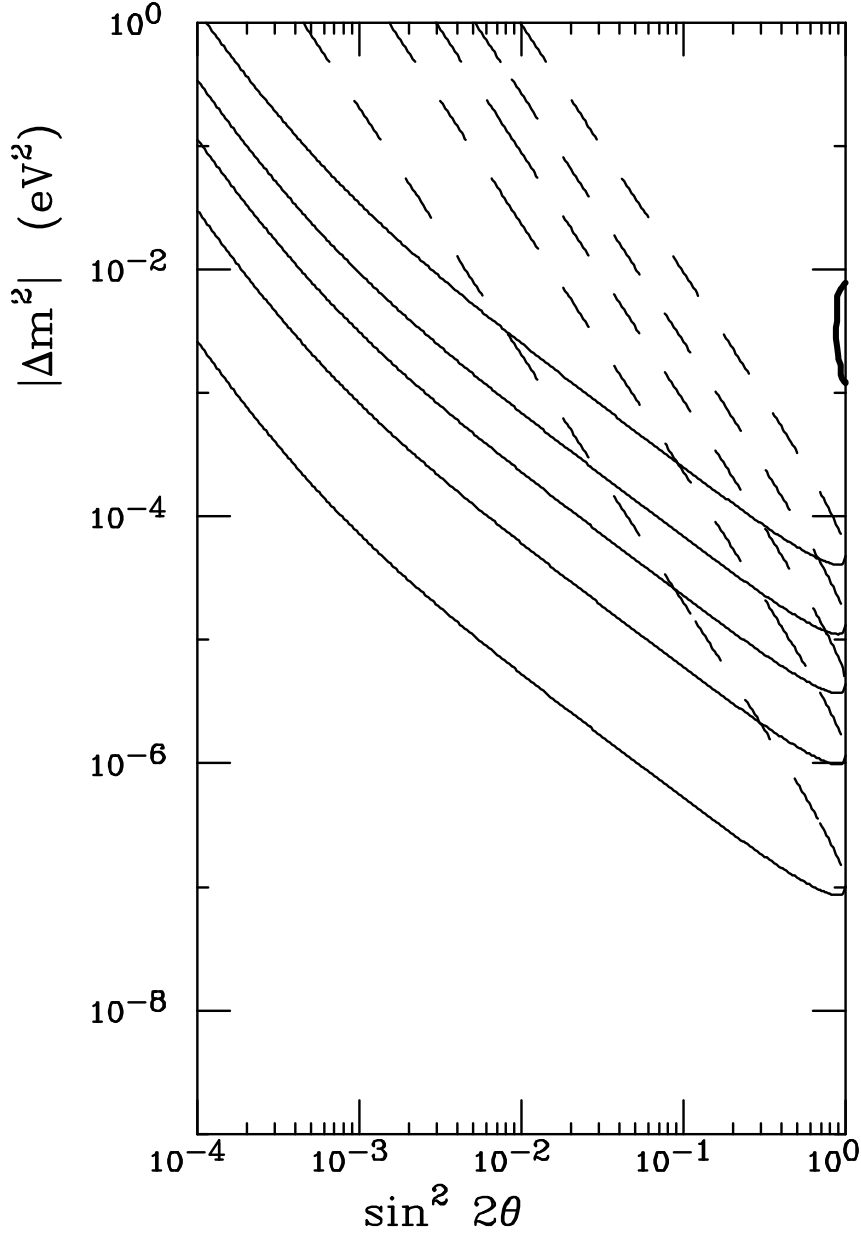


Figure 4: Lines in the plane  $(s^2, |\delta m^2|)$  that correspond to a fixed value of the sterile neutrino effective number  $N_{\nu_s}^{\text{eff}}$ : 0.1, 0.3, 0.5, 0.7, 0.9 (from bottom up). The curves are calculated assuming that the asymmetry of the medium remains negligibly small. The solid (dashed) lines correspond to  $\delta m^2 < 0$  ( $\delta m^2 > 0$ ). The thick solid line shows the allowed region indicated by the Super-Kamiokande experimental results.

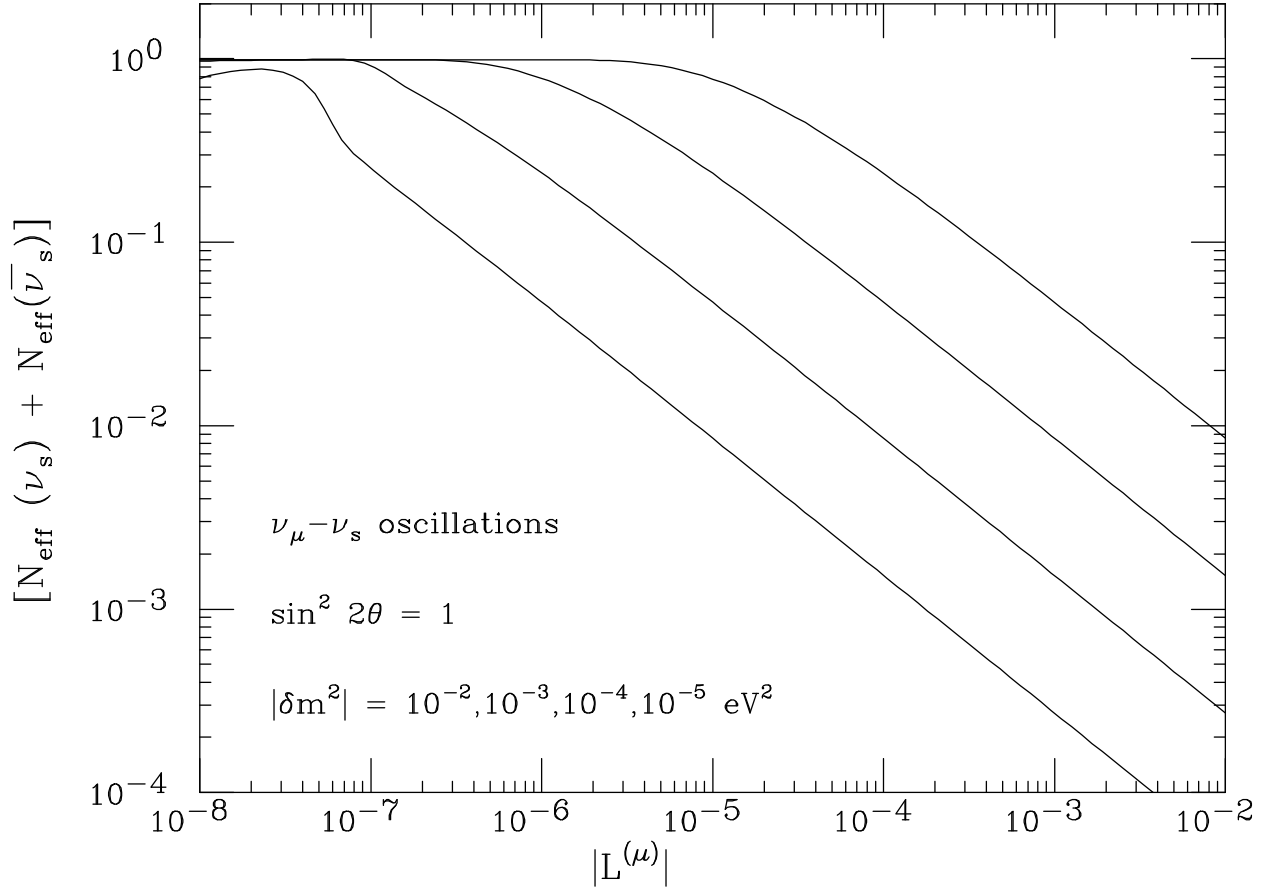


Figure 5: Plot of the effective number of sterile neutrinos  $N_{\nu_s}(\text{eff})$  as a function of  $L^{(\mu)}$  calculated assuming that the sterile neutrino is maximally mixed with a muon (or a tau) neutrino. The curves are calculated for  $|\delta m^2| = 10^{-2}, 10^{-3}, 10^{-4}$  and  $10^{-5} \text{ eV}^2$  (from right to left). In the calculation the asymmetry  $L^{(\mu)}$  is fixed and it is not considered as a dynamical variable.

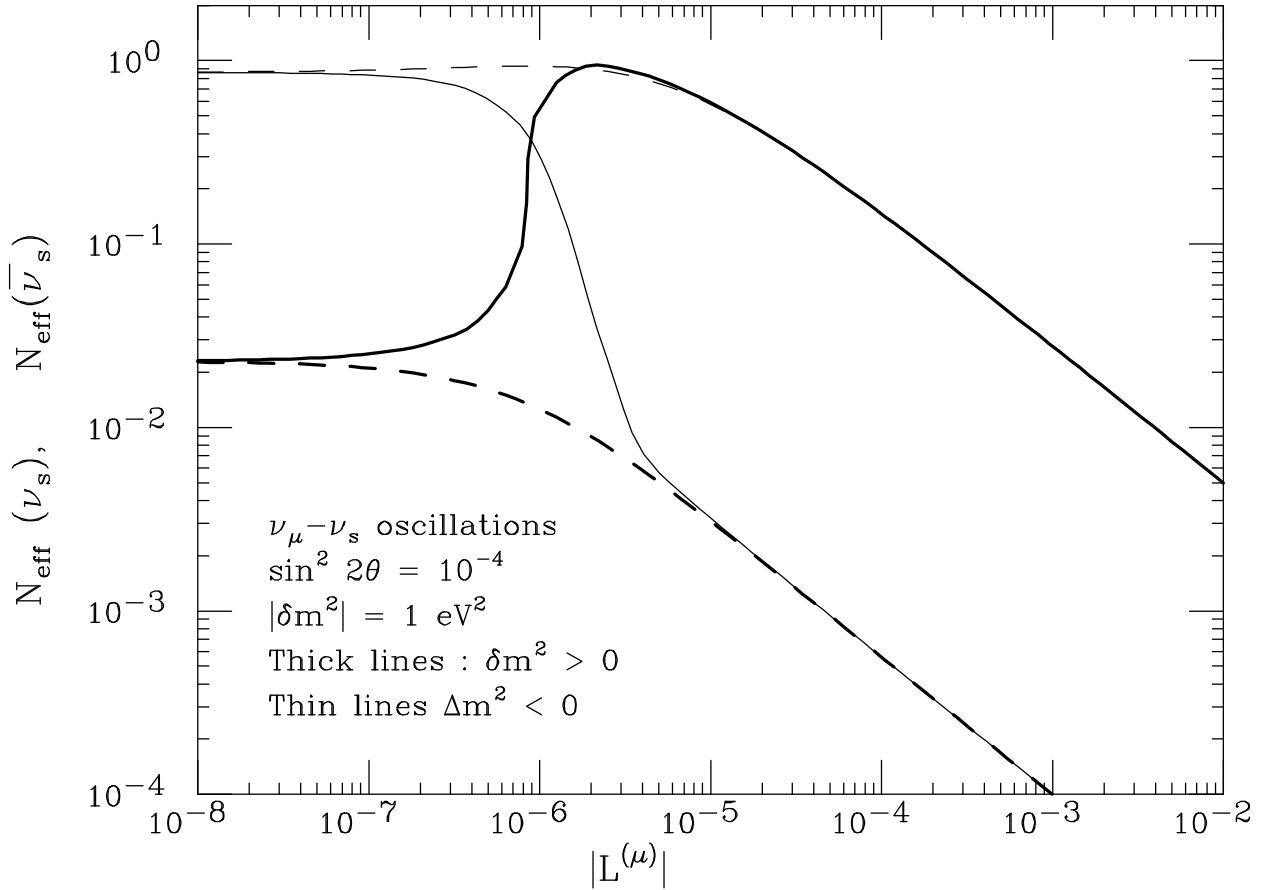


Figure 6: Plot of the effective number of sterile neutrinos  $N_{\nu_s}(\text{eff})$  as a function of  $L^{(\mu)}$  calculated assuming that the sterile neutrino is mixed with a muon (or a tau) neutrino with  $s^2 = 10^{-4}$  and  $|\delta m^2| = 1 \text{ eV}^2$ . The thick (thin) lines correspond to  $\delta m^2 > 0$  ( $\delta m^2 < 0$ ). The solid (dashed) curves correspond to neutrinos (antineutrinos) for  $L^{(\mu)} > 0$  and vice versa for  $L^{(\mu)} < 0$ . In the calculation the asymmetry  $L^{(\mu)}$  is fixed and it is not considered as a dynamical variable.

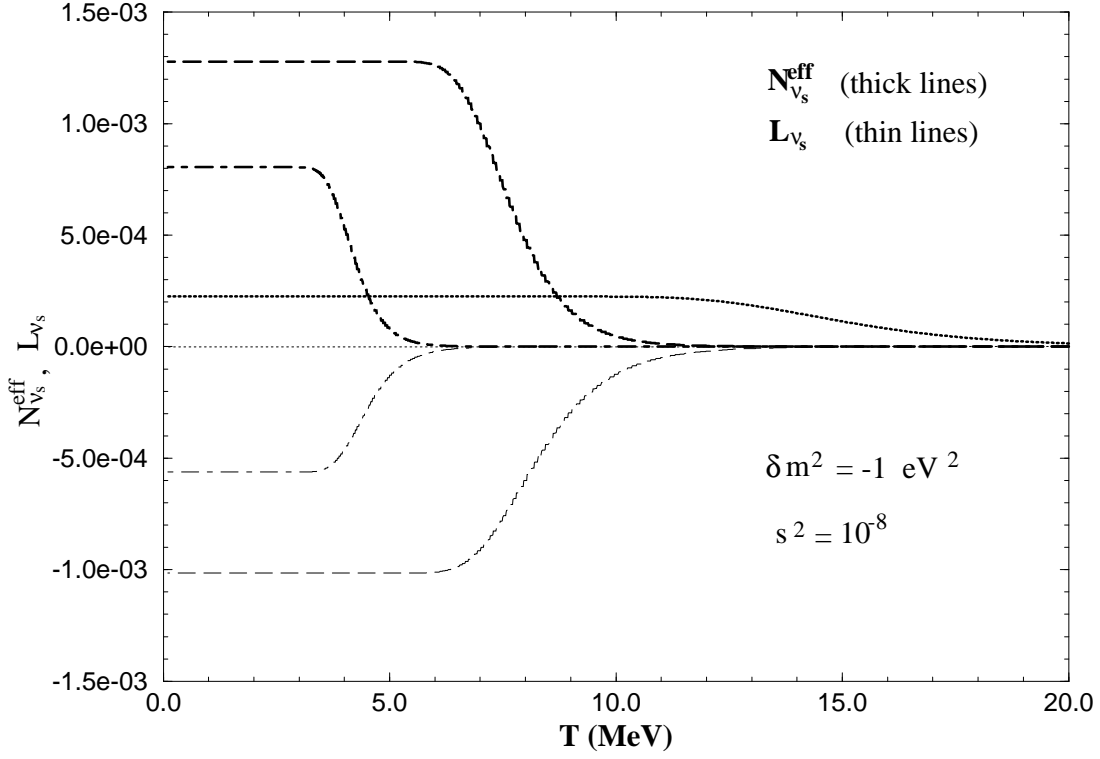


Figure 7: Evolution with temperature of the density  $N_{\nu_s}^{\text{eff}}$  and asymmetry  $L_{\nu_s}$  of sterile neutrinos, calculated assuming the existence of  $\nu_s \leftrightarrow \nu_{\mu(\tau)}$  oscillations with  $\delta m^2 = -1 \text{ eV}^2$  and  $s^2 = 10^{-8}$ , and a time independent value for the charge asymmetry of the medium. The thick (thin) lines describe the evolution of  $N_{\nu_s}^{\text{eff}}$  ( $L_{\nu_s}$ ). The dotted lines correspond to  $L^{(\mu)} = 0$ , the dashed to  $L^{(\mu)} = 10^{-5}$  and the dot-dashed ones to  $L^{(\mu)} = 10^{-4}$ . For  $L^{(\mu)} = 0$ ,  $\nu$ 's and  $\bar{\nu}$ 's oscillate in the same way and no asymmetry is generated. For non negligible values of  $L^{(\mu)}$  the sterile antineutrino production can be enhanced, and an asymmetry is generated.

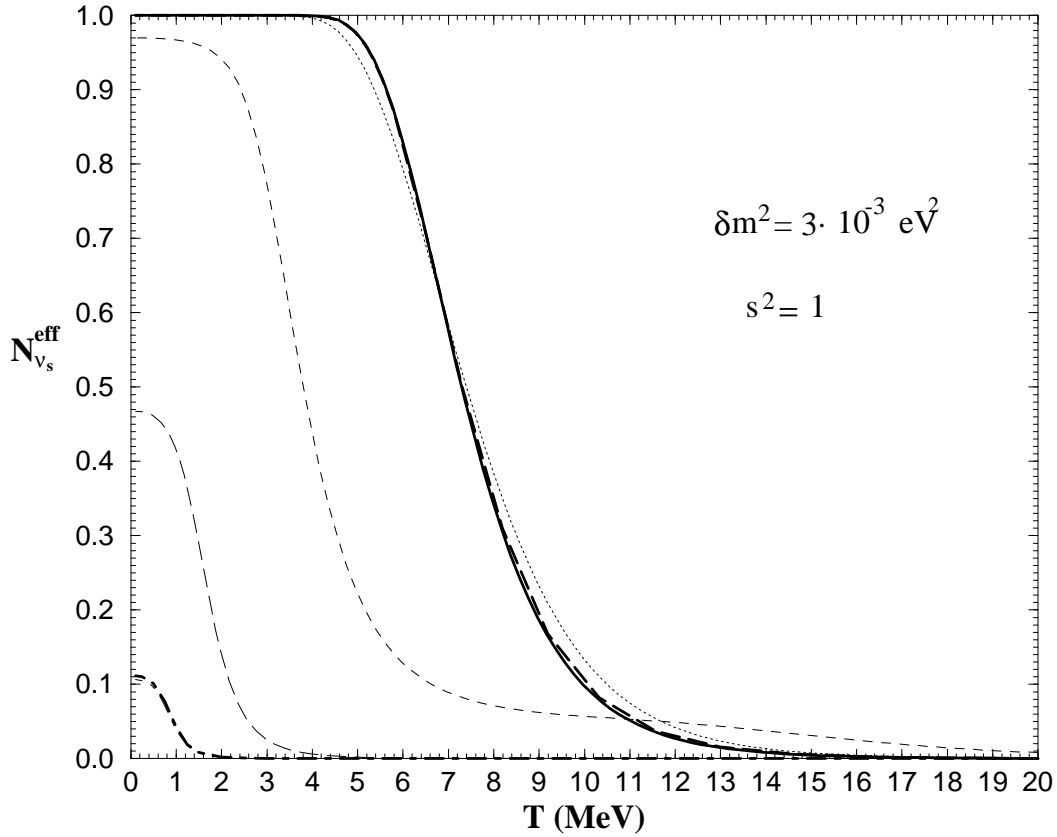


Figure 8: Evolution of the sterile neutrino energy density calculated assuming the existence of  $\nu_{\mu(\tau)} \leftrightarrow \nu_s$  oscillations with maximal mixing and  $\delta m^2 = 3 \times 10^{-3} \text{ eV}^2$ . The solid, dotted, dashed, long dashed and dot-dashed lines correspond to an initial value  $L_{in}^{(\alpha)} = 0, 10^{-7}, 10^{-6}, 10^{-5}$  and  $10^{-4}$ . The thin lines are calculated considering  $L^{(\alpha)}$  as a constant, the thick lines taking into account the dynamical evolution of  $L^{(\alpha)}$ .

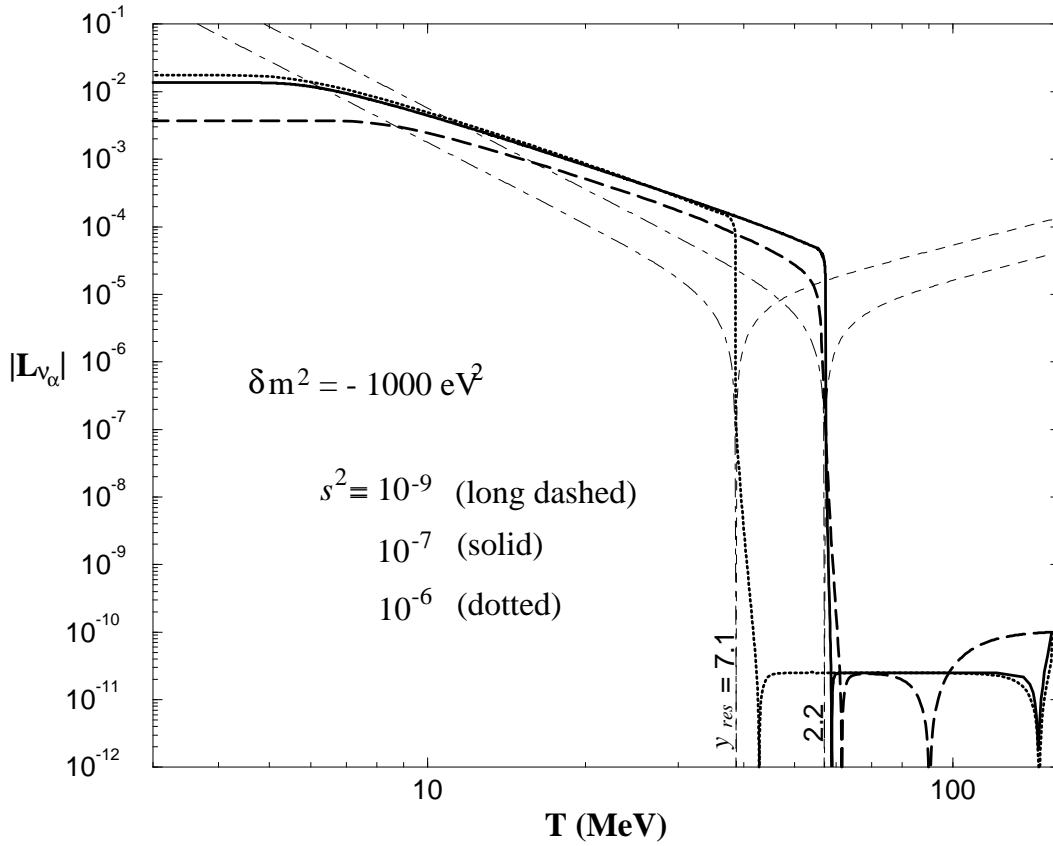


Figure 9: Evolution with temperature of the lepton number  $L_{\nu_\alpha}$  ( $\alpha = \mu, \tau$ ) (thick lines) calculated assuming the existence of  $\nu_s \leftrightarrow \nu_{\mu(\tau)}$  oscillations with the indicated oscillation parameters. The evolution of the neutrino populations is started at  $T = 150$  MeV with  $L^{(\alpha)} = 10^{-10}$  and  $\tilde{\eta} = 5 \times 10^{-11}$ . The thin lines are the resonance curves for the indicated values of momenta (dashed for neutrinos and dot-dashed for antineutrinos).



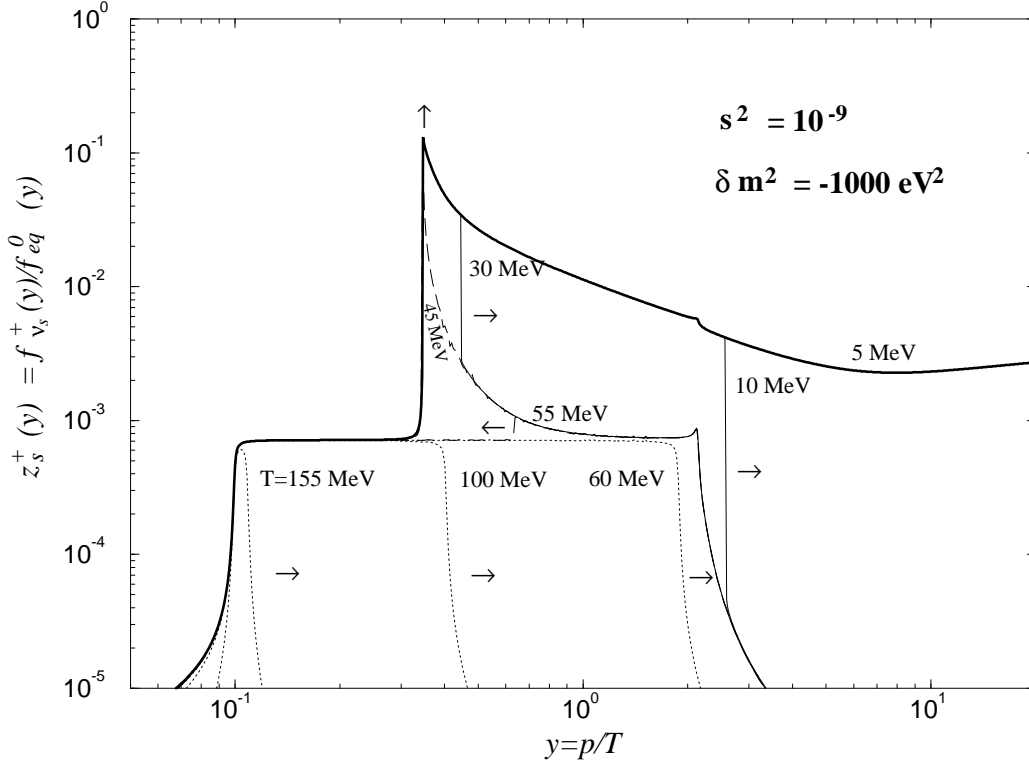


Figure 10: Evolution of the sterile neutrino distribution with temperature for  $\nu_s \leftrightarrow \nu_{\mu(\tau)}$  oscillations when lepton number is generated. The oscillation parameters are  $\delta m^2 = -1000 \text{ eV}^2$  and  $s^2 = 10^{-9}$  and correspond to the thick long-dashed line in figure 9. The different curves correspond to increasing temperature. Above the critical temperature ( $T_c \sim 60 \text{ MeV}$ ) a standard production with zero lepton number occurs, up to  $y^{\text{res}} \simeq 2.2$ . At lower temperature, an enhancement regime with constant  $y^{\text{res}} \simeq 0.35$  is clearly apparent. The production occurring after lepton number generation gives a dominant contribution in this case, but the total production is anyway too small to be relevant for BBN bounds.

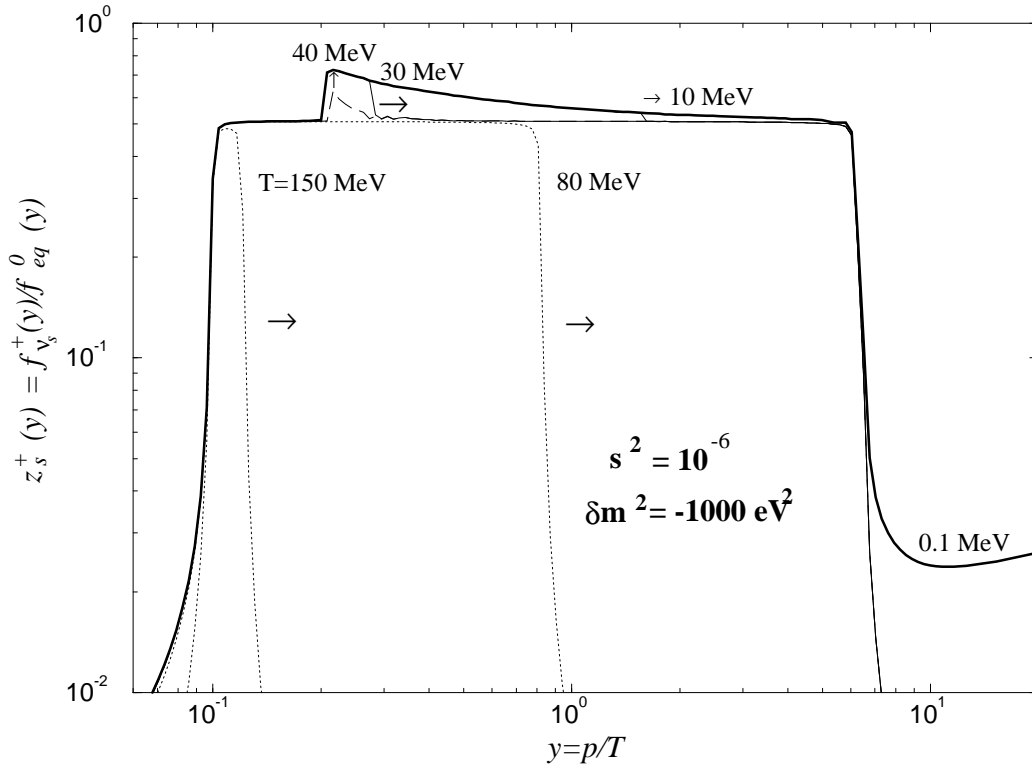


Figure 11: Evolution of the sterile neutrino distribution with temperature for  $\nu_s \leftrightarrow \nu_{\mu(\tau)}$  oscillations when lepton number is generated. The oscillation parameters are  $\delta m^2 = -1000 \text{ eV}^2$  and  $s^2 = 10^{-6}$  and correspond to the thick dotted line in figure 9. The different curves correspond to increasing temperature. Above the critical temperature ( $T_c \sim 42 \text{ MeV}$ ) a standard production with zero lepton number occurs. It can be noticed that in this case  $y^{\text{res}} \simeq 7.1$ , since  $z_s^+ \lesssim 1$ . The enhancement regime now is too short to be observed and the dominant contribution to the total production comes from the standard regime with zero lepton number.

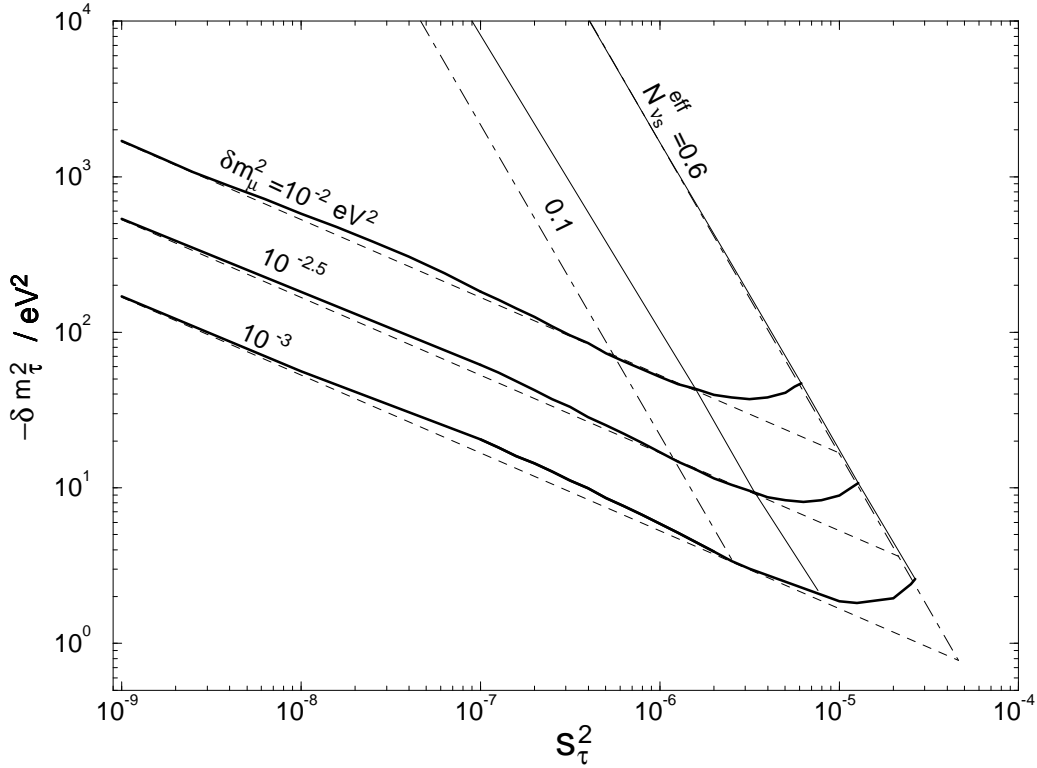


Figure 12: Lines corresponding to constant  $N_{\nu_s}^{\text{eff}}$  in the plane  $(s_\tau^2, \delta m_\tau^2)$ . The thin solid lines correspond to  $N_{\nu_s}^{\text{eff}} = 0.1$  and  $0.6$ ; the thin dot-dashed lines correspond to the same values of  $N_{\nu_s}^{\text{eff}}$  and have been calculated in a two neutrino mixing framework with negligible  $L^{(\tau)}$ . The three thick solid lines, calculated for the three values  $\delta m_\mu^2 = 10^{-3}$ ,  $10^{-2.5}$  and  $10^{-2}$  eV<sup>2</sup>, correspond to the points where the energy density of sterile neutrinos passes quasi-discontinuously from the value  $N_{\nu_s}^{\text{eff}} = 1$  (below the curve) to a much lower value (above the curve). The three dashed lines, corresponding to equation (83), give a first approximation description of the numerical results.

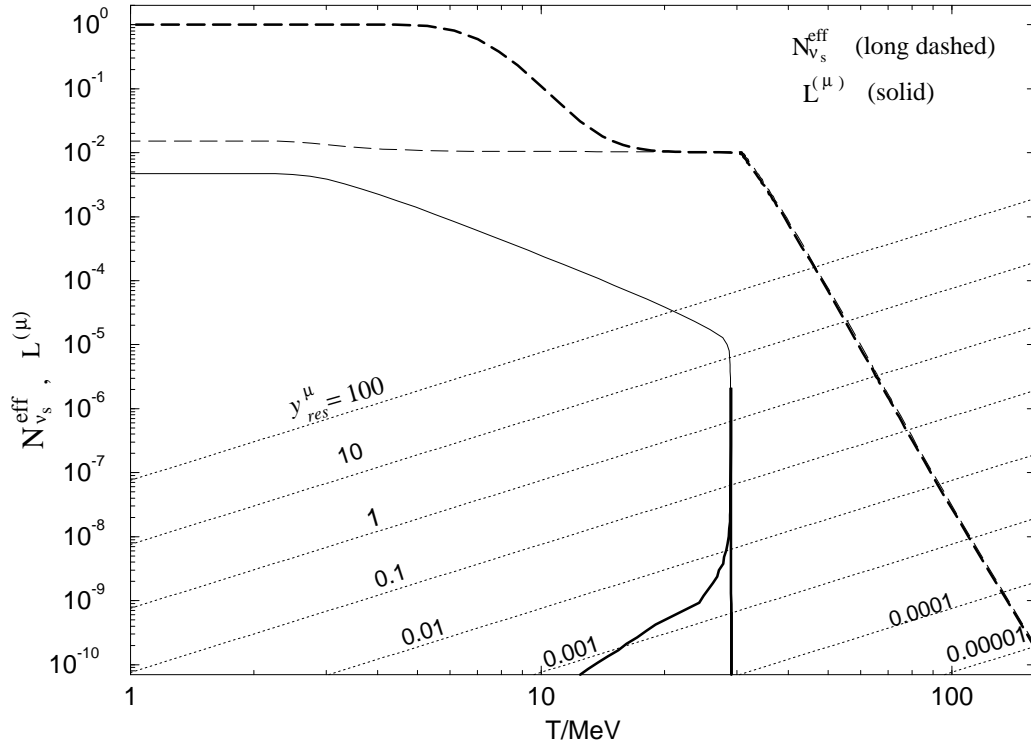


Figure 13: Evolution the asymmetry  $L^{(\mu)}$  (solid lines) and the sterile neutrino energy density  $N_{\nu_s}^{\text{eff}}$  (dashed lines) as a function of the temperature. The thin curves are calculated for the set oscillation parameters  $\delta m_\mu^2 = 10^{-2.5} \text{ eV}^2$ , and  $s_\tau^2 = 10^{-6}$ , and  $\delta m_\tau^2 = 17.80 \text{ eV}^2$ , The thick curves are calculated for the same values of  $\delta m_\mu^2$  and  $s_\tau^2$  but with a slightly smaller value  $\delta m_\tau^2 = 17.40 \text{ eV}^2$ .

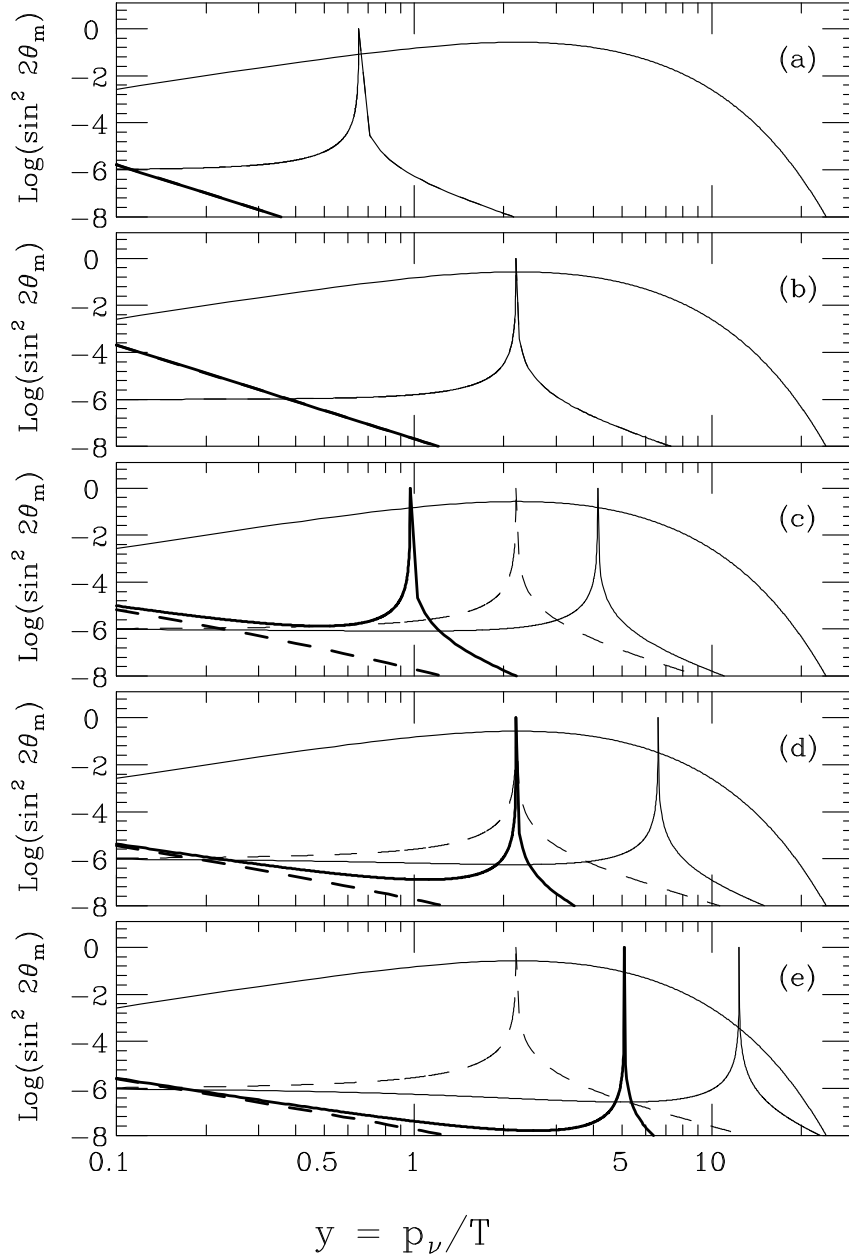


Figure 14: Mixing parameters of  $\nu$ 's and  $\bar{\nu}$ 's in matter for different conditions of the medium. The oscillation parameters are:  $\delta m_\mu^2 = 10^{-3} \text{ eV}^2$ ,  $s_\mu^2 = 1$ ,  $\delta m_\tau^2 = -10 \text{ eV}^2$ ,  $s_\tau^2 = 10^{-6}$ . The 4 panels refer to the situations: (a)  $T = 58.1 \text{ MeV}$ ,  $L_{\nu_\tau} = 0$ , (b)  $T = 38.7 \text{ MeV}$ ,  $L_{\nu_\tau} = 0$ , (c)  $T = 34.9 \text{ MeV}$ ,  $L_{\nu_\tau} = 8.9 \times 10^{-7}$ , (d)  $T = 32.2 \text{ MeV}$ ,  $L_{\nu_\tau} = 1.7 \times 10^{-6}$ , (e)  $T = 29.1 \text{ MeV}$ ,  $L_{\nu_\tau} = 3.2 \times 10^{-6}$ ; in all cases  $L_{\nu_\mu} \simeq 0$ . In each panel the thick (thin) curves refer to  $\nu_\mu \leftrightarrow \nu_s$  ( $\nu_\tau \leftrightarrow \nu_s$ ) oscillations, the solid (dashed) lines to neutrinos (antineutrinos). The thin, smooth curve is a plot of the function  $y^2 f_{eq}^0(y)$ .